"Chaotic" dart leaders in triggered lightning: Electric fields, X-rays, and source locations

Jonathan D. Hill,[1] Martin A. Uman,[1] Douglas M. Jordan,[1] Joseph R. Dwyer,[2] and Hamid Rassoul[2]

Received 19 August 2011; revised 30 November 2011; accepted 1 December 2011; published 14 February 2012.

[1] We present the first published observations of "chaotic" dart leaders in triggered-lightning discharges. We examine four leaders that exhibited "chaotic" electric field derivative (dE/dt) signatures in their final 10 to 12 μs. The dE/dt signatures were characterized by bursts exhibiting widths of the order of hundreds of nanoseconds on which were superimposed irregular pulses with widths of the order of tens of nanoseconds. These unique signatures were dissimilar from the dE/dt waveforms observed from dart or dart-stepped leaders in triggered lightning. Three-dimensional locations for dE/dt pulses that radiated from the bottom 200 m of the leader channels were determined, as were emission times. Vertical leader speeds for the four "chaotic" dart leaders were estimated to range from 2.0 to 4.3 $\times$ 10^7 m/s. A relatively continuous flux of energetic radiation (X-rays and gamma rays) was observed during the final 10–13 μs of each "chaotic" dart leader. Some individual photons had energies more than 1 MeV. High-speed video images of three "chaotic" dart leaders were obtained at a frame rate of 300 kilo-frames per second (exposure time of 3.33 μs). One image, in the frame immediately prior to the return stroke, shows an upward positive leader 11.5 m in length propagating from the launch facility and a downward negative leader above with a streamer zone length of about 25 m. Channel base currents preceding the four "chaotic" dart leaders were of unusually long duration and large charge transfer, and return strokes following them had larger than usual peak currents.

Citation: Hill, J. D., M. A. Uman, D. M. Jordan, J. R. Dwyer, and H. Rassoul (2012), "Chaotic" dart leaders in triggered lightning: Electric fields, X-rays, and source locations, *J. Geophys. Res.*, *117*, D03118, doi:10.1029/2011JD016737.

1. Introduction

[2] The electromagnetic emissions of descending negatively charged dart leaders and dart-stepped leaders preceding subsequent return strokes in natural and triggered lightning have been well studied [e.g., *Schonland et al.*, 1935; *Krider et al.*, 1977; *Orville and Idone*, 1982; *Guo and Krider*, 1985; *Jordan et al.*, 1992; *Wang et al.*, 1999b]. References in the literature to the "chaotic" leader process are relatively few [e.g., *Weidman*, 1982; *Bailey et al.*, 1988; *Willett et al.*, 1990; *Rakov and Uman*, 1990; *Izumi and Willett*, 1993; *Davis*, 1999; *Gomes et al.*, 2004; *Mäkelä et al.*, 2007; *Lan et al.*, 2011]. Furthermore, the term "chaotic" leader is not well defined but has, in general, been used to refer to a relatively continuous sequence of irregular electric field pulses occurring within the roughly 2 ms preceding a subsequent return stroke in natural lightning. These pulses are different from the more well-documented dart-stepped leader pulses. In his PhD dissertation, *Weidman* [1982, p. 77] was the first to use the term "chaotic" to differentiate the newly identified leader process from the dart or dart-stepped leader process. *Weidman* [1982], in his Figures 3.17b and 3.17c, shows two leader electric field derivative (dE/dt) waveforms, demonstrating an irregular sequence of pulses in the final 22 μs prior to the return stroke, that are clearly different from the dart-stepped leader record in his Figure 3.17a. The causative discharges occurred mostly over salt water at distances of 10 to 60 km from the measuring station located on Anna Maria Island near the southern entrance to Tampa Bay, Florida. *Bailey et al.* [1988] reported on four events termed "chaotic subsequent strokes" with similar rapidly varying irregular pulses immediately prior to the onset of the return stroke in the dE/dt waveforms. The discharges occurred over salt water at distances from 15 to 45 km from the measuring station located at the Kennedy Space Center in Florida. They also found that "chaotic subsequent strokes" produced larger positive and negative peak dE/dt (return stroke) signatures than those preceded by normal dart leaders or dart-stepped leaders. *Willett et al.* [1990] recorded 15 events classified as "chaotic" leaders from three storms at ranges less than 35 km using the equipment described by *Bailey et al.* [1988]. In

[1]Department of Electrical and Computer Engineering, University of Florida, Gainesville, Florida, USA.
[2]Department of Physics and Space Sciences, Florida Institute of Technology, Melbourne, Florida, USA.

0148-0227/12/2011JD016737

their Figure 1, they give a "chaotic" leader dE/dt waveform showing an irregular pulse sequence similar to those reported by *Weidman* [1982] and *Bailey et al.* [1988]. The pulse sequence extends backward in time to at least 60 μs before the return stroke. *Rakov and Uman* [1990] analyzed 15 subsequent return strokes with preceding "chaotic" leader signatures in 76 close, over land, negative cloud-to-ground lightning discharges containing a total of 270 subsequent return strokes. The data were recorded near Tampa, Florida. Similar to the results of *Bailey et al.* [1988], they reported that the "chaotic" leaders are more likely to precede the larger peak electric field return strokes in a given flash. They suggest that the irregular pulse signature of the "chaotic" leader could be associated with an unknown stepping process of a dart leader that had previously moved continuously downward along the preconditioned channel, and they also propose that the "chaotic" leader process might be related to the electromagnetic interaction between the simultaneously propagating downward-moving, negatively charged leader channel and the upward-moving, positively charged connecting leader channel. Perhaps the most thorough analysis of the "chaotic" leader process is found in the PhD dissertation of *Davis* [1999]. A total of 12 "chaotic" leaders were recorded in 16 negative cloud-to-ground lightning discharges at the Kennedy Space Center, Florida. Time of arrival (TOA) techniques were employed to locate dE/dt sources in three dimensions from a five station network of flat-plate antennas covering an area of 15 $\times$ 15 km. The average leader speeds for two "chaotic" leader events were calculated to be 3.2 $\times$ 10^7 m/s and 5.0 $\times$ 10^7 m/s, respectively, speeds higher than those typically associated with dart-stepped leaders and in better agreement with the speeds of dart leaders. For two "chaotic" leader events, the median interpulse intervals were determined to be 0.9 μs and 1.45 μs, respectively, for a threshold 4.4% above the background noise level. A total of eight "chaotic" leader waveforms are shown, with durations varying from a few tens of microseconds to about 180 μs. Of particular interest is the bottom dE/dt trace from *Davis* [1999, p. 111]. What appears as a typical dart-stepped leader for the first 870 μs of the record (accounting for a 30 μs dead time between each recording) transitions into a "chaotic" leader in at least the final 180 μs before the return stroke. *Gomes et al.* [2004] recorded chaotic pulse trains (CPT) in 95 of the 169 lightning discharges they recorded in Sweden, Denmark, and Sri Lanka. The authors chose to use the term "chaotic pulse train" as opposed to "chaotic" leader or "chaotic subsequent stroke" because, in several cases, they observed irregular sequences of pulse activity independent of subsequent return strokes. The causative storms were 10 to 150 km distant. It was reported that CPTs immediately preceding subsequent return strokes had pulse widths generally in the range from 2 to 4 μs (measured as short as 400 ns), interpulse intervals from 2 to 20 μs, and mode value duration of 400 to 500 μs. *Mäkelä et al.* [2007] also performed an analysis of "chaotic" leaders in Sri Lanka using both a wideband (upper frequency limit of about 12 MHz) flat-plate electric field antenna and a vertical antenna tuned to a resonant frequency of 10.44 MHz with a bandwidth of 2.02 MHz. They analyzed 34 lightning flashes containing 74 subsequent return strokes, more than 30% of which appeared to be preceded by "chaotic" leaders. The discharges were estimated to occur at distances from 1 to 7 km from the measuring station. They reported that the "chaotic" component during the leader phase had an average duration of about 300 μs but rarely exceeded 500 μs. Using the narrowband HF data, they also found that the HF intensity of individual peaks of the "chaotic" component, present during the leader phase preceding a subsequent return stroke, can approach the intensity level recorded from the actual return stroke, in stark contrast to the typically weak emission from both dart and dart-stepped leaders. *Lan et al.* [2011] analyzed 210 return strokes in 74 negative cloud-to-ground flashes in China. They reported that 48% of the subsequent return strokes in the study were preceded by a chaotic component (referred to as CPT) with an average duration of 472 μs. The widths of individual CPT pulses were found to range from 0.5 to 8 μs. From two-station interferometer measurements, the propagation velocities of the downward leaders associated with CPT were found to be about 2.0 $\times$ 10^7 m/s.

[3] In this article, we present the first published "chaotic" dart leader waveforms associated with triggered-lightning return strokes, which are similar to natural lightning subsequent return strokes. In the previous studies of "chaotic" leaders preceding natural subsequent return strokes, no detailed analysis was performed of the characteristics of the sub-microsecond irregular field variations. We examine in detail the sub-microsecond field variations of two "chaotic" dart leaders within 6 μs of the return stroke and within about 200 m from the ground, establishing new terminology to describe the slower background field changes of the order of hundreds of nanoseconds and the faster field variations of the order of tens of nanoseconds superimposed on the slower background field changes. We also provide measured statistics for the pulse width of the slower background field changes and pulse width and amplitude for the faster superimposed field variations. Finally, we adopt the term "chaotic" dart leader instead of previously used terms because the overall characteristics of the leader process closely resemble those of a typical dart leader with superimposed irregular sequences of pulses in the electric field derivative signature observed in the bottom 200 m of the leader channel.

[4] Measurements from ground-based energetic radiation detectors have shown that roughly 80% of dart and dart-stepped leaders preceding rocket triggered–lightning return strokes emit detectable energetic radiation (primarily X-rays and gamma rays) when they are within several hundred meters of ground, that is, within a few hundred microseconds of the subsequent return stroke initiation [e.g., *Dwyer et al.*, 2003, 2004, 2011; *Saleh et al.*, 2009]. Using TOA techniques, *Howard et al.* [2008] showed that the high-frequency electric field sources emitted from a descending negatively charged dart-stepped leader preceding a rocket triggered–lightning return stroke were both in close spatial proximity (less than 50 m) and temporal relation (0.1 to 1.3 μs preceding) to the corresponding X-ray sources. In this article, we present the first measurements of energetic radiation specifically associated with "chaotic" dart leader processes and also compare the emissions to those radiated by typical dart and dart-stepped leaders preceding rocket triggered–lightning return strokes.

[5] Finally, we provide high-speed video images of two "chaotic" dart leaders within 140 m of the ground and

Figure 1. Satellite image of the ICLRT showing LF1 and LF2, the data acquisition trailer, dE/dt and energetic radiation sensor locations, and the Photron high-speed camera location.

compare the optical characteristics to those recorded for dart and dart-stepped leaders.

2. Experiment

[6] The electric field, energetic radiation (X-rays and gamma rays), and high-speed photographic measurements described in this article were obtained during the summer of 2010 at the International Center for Lightning Research and Testing (ICLRT) located on the Camp Blanding Army National Guard base in north-central Florida. Lightning was artificially initiated (triggered) by launching a 1 m fiberglass rocket carrying a 700 m spool of 32 AWG Kevlar-coated copper wire toward a region of high negative charge concentration produced by an overhead or nearby thunderstorm. The end of the wire spool was connected to the grounded rocket launcher. A detailed description of the triggered-lightning process is given by *Rakov and Uman* [2003, chap. 7]. Lightning return strokes were triggered to two structures: (1) an aluminum rocket launcher located on top of a 11 m wooden tower, and (2) a copper-clad steel intercepting rod located 14 m above a rocket launcher placed on the ground surface. In the first launching configuration, hereafter referred to as launching facility 1 (LF1), the rocket launcher was grounded directly to a single 25 m copper-clad steel ground rod. In the second launching configuration, hereafter referred to as launching facility 2 (LF2), the intercepting rod was grounded through nine 12 m copper-clad steel ground rods connected in parallel and separated by tens of meters. In both the launching configurations, current was measured immediately below the strike object, the rocket launcher in the LF1 configuration and the intercepting rod in the LF2 configuration, with a noninductive T&M Research R-7000-10 current viewing resistor (CVR) having a bandwidth from DC to 8 MHz. An overhead map of the ICLRT is shown in Figure 1 with annotations for both launching facilities and the locations of all dE/dt sensors and energetic radiation detectors.

[7] Electric field derivative (dE/dt) waveforms were recorded at ten distances from the lightning channel base ranging from 37 to 443 m with flat-plate antennas of area 0.155 m^2. The −3 dB bandwidth of the antenna response is about 40 MHz (determined by the antenna capacitance and the load impedance), but the received signals are bandwidth limited to 20 MHz by the fiber-optic data transmission system and the antialiasing filter at the digital storage oscilloscope input. A thorough description of the dE/dt antennas used at the ICLRT can be found in the PhD dissertation of *Jerauld* [2007]. The ten dE/dt antennas comprise a small-area (around 0.25 km^2) TOA network, similar to that described by *Howard et al.* [2008, 2010], capable of locating high-frequency electric field sources in three dimensions with high spatial and temporal resolution when the sources are within about 500 m of the ground. The dE/dt sources near the center of the TOA network with altitudes greater than about 50 m are typically located with errors of less than one meter in both the lateral plane and altitude. For lower sources, the lateral location errors remain on the order of 1 m, while the altitude errors increase to several meters. Sources are located spatially and temporally by using the signal arrival times at each available station (imposing a $N \geq 5$ threshold), derived from measurement of the peak dE/dt with 4 ns accuracy, the sampling resolution of the system, as input to a nonlinear least squares Marquardt algorithm similar to that described by *Thomas et al.* [2004] and *Koshak et al.* [2004]. Actual signal arrival times are calculated by

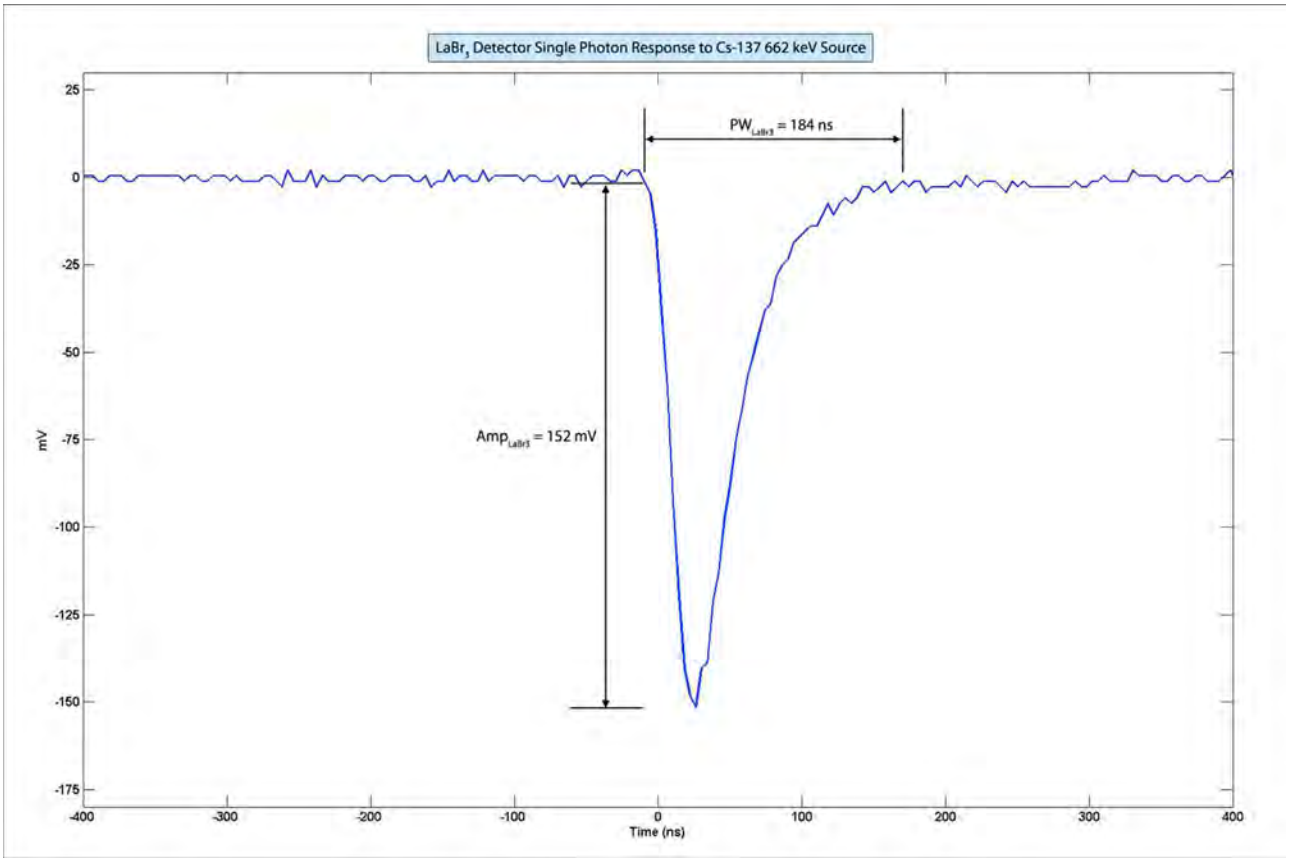

Figure 2. $LaBr_3$/PMT detector single photon response to a Cs-137 662 keV source. Typical amplitude and full pulse width are annotated.

removing the artificial propagation delays introduced by coaxial and fiber-optic cable runs from each sensor to the oscilloscope inputs. The propagation delays are measured with an accuracy greater than the sampling resolution of the system.

[8] Energetic radiation measurements were colocated within 10 m of each dE/dt sensor. Two lanthanum bromide ($LaBr_3$), eight sodium iodide (NaI), and eight 1 m^2 plastic scintillation devices were employed. The $LaBr_3$ and NaI detectors were each mounted to a photomultiplier tube (PMT). Two PMTs were mated to opposite sides of each plastic scintillator. The $LaBr_3$ and NaI detectors were calibrated using a 662 keV Cs-137 gamma ray source. A plot of the $LaBr_3$/PMT detector single photon response to the calibration source in given in Figure 2. The typical amplitude response of the sensor to the calibration source is 152 mV and the typical full pulse width is 184 ns. The spatial positions of all dE/dt sensors and energetic radiation detectors were measured to an accuracy of 1 cm to the center of the sensor using a Differential Global Positioning System (DGPS) for the lateral coordinate measurements and a closed-level loop for the altitude coordinate measurements. State plane coordinate measurements were based on the Florida North NAD83 data. The coordinates were converted to a local coordinate system with origin at the far southwest corner of the ICLRT. All altitude measurements are referenced to the local coordinate system origin.

[9] Video images of the triggered-lightning discharges were acquired from a distance of 430 m (LF1), as shown in Figure 1, using a Photron SA1.1 high-speed camera operated at a frame rate of 300 kilo-frames per second (kfps). A 20 mm Nikon lens was mounted to the camera and was set to an aperture of F/4. This setup provided a spatial resolution of 0.43 m/pixel and a total vertical field of view of 138 m. The camera was configured to record a pixel region measuring 320 × 32 (vertical × horizontal) with a 12-bit gray scale amplitude resolution.

[10] With the exception of one $LaBr_3$ detector, all dE/dt and energetic radiation measurements were transmitted to a central shielded data acquisition trailer via Opticomm MMV-120C FM fiber-optic links (nominal bandwidth DC-20 MHz, −3 dB). The output from the single $LaBr_3$/PMT detector was transmitted directly over approximately 20 m of double-shield coaxial cable to achieve higher bandwidth and signal-to-noise ratio. The coaxial cable was enclosed in a wire braid for additional electromagnetic shielding. All signals were digitized at a sampling rate of 250 MS/s by LeCroy Waverunner 44 Xi or LeCroy Waverunner LT344 oscilloscopes with 8-bit amplitude resolution. The Waverunner 44 Xi oscilloscopes were operated in segmented memory mode and were capable of recording 10 segments, each of 5 ms length. The Waverunner LT344 oscilloscopes also operated in segmented memory mode but recorded only 2 segments, each of 2 ms length. Only the outputs of the eight NaI/PMT detectors were digitized on the Waverunner LT344. The segments for all oscilloscopes were configured to record with 50% pretrigger. The

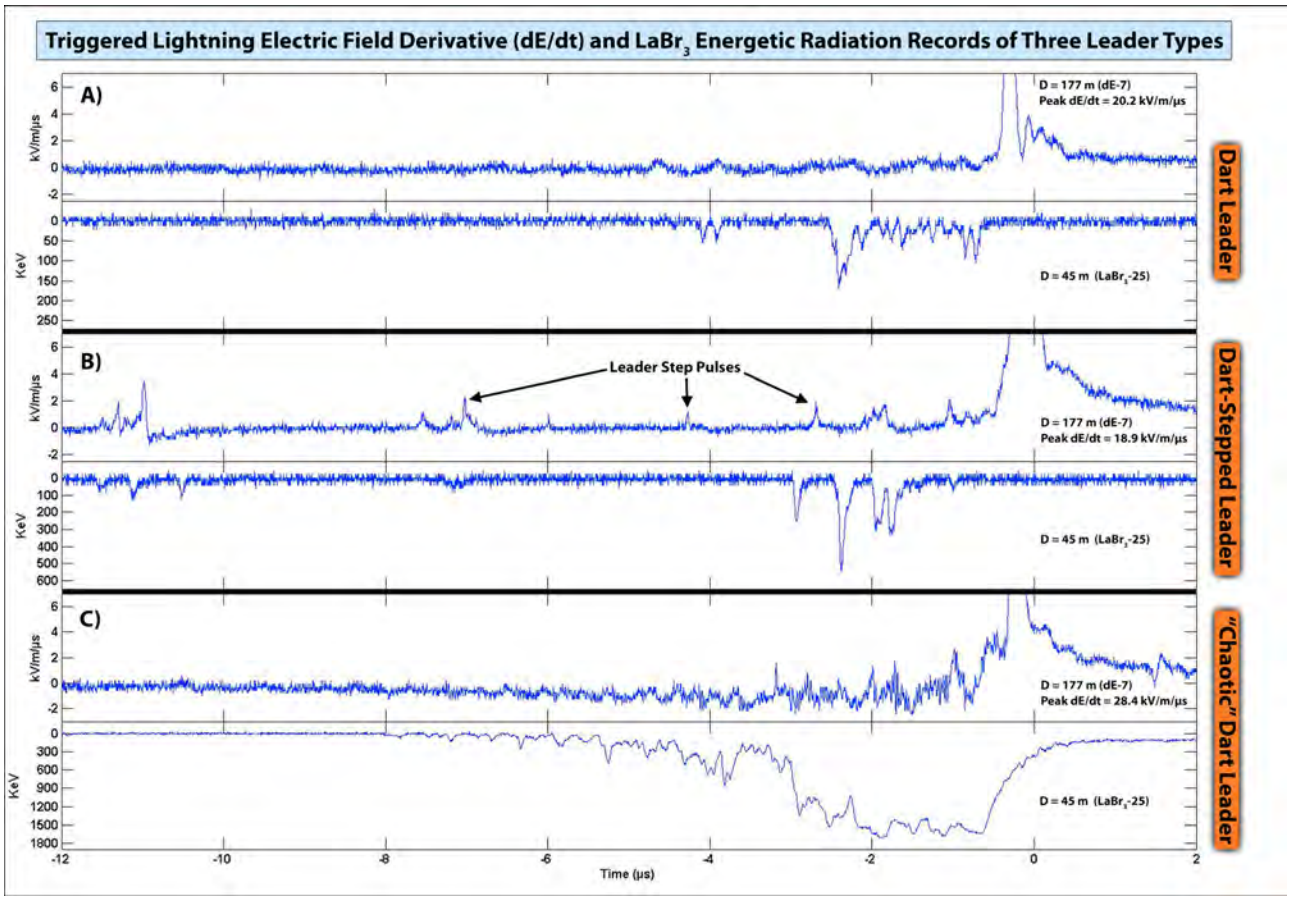

Figure 3. Electric field derivative (dE/dt) and $LaBr_3$ energetic radiation records of (a) dart leader, (b) dart-stepped leader, and (c) "chaotic" dart leader preceding rocket triggered–lightning return strokes.

data acquisition system and high-speed camera were triggered to begin recording when the current measured at the lightning channel base exceeded a threshold of about 6 kA.

3. Background and Overall Characteristics

[11] To describe the "chaotic" dart leader process appropriately, we first needed to develop criteria to differentiate "chaotic" dart leaders from typical dart leaders and dart-stepped leaders preceding triggered-lightning return strokes. In Figure 3, we show, on a 14 μs scale, dE/dt and associated energetic radiation waveforms corresponding to the three classifications of leader types. The vertical scales of all three dE/dt measurements have been truncated to better show the lower amplitude field changes occurring during the leader phases. The peak dE/dt measured in association with each subsequent return stroke is given for reference. The three dE/dt measurements were measured 177 m from the triggered-lightning channel base, and the three corresponding energetic radiation measurements were recorded with a $LaBr_3$/PMT detector 45 m from the lightning channel base. A typical dart leader dE/dt waveform is shown in Figure 3a. The dart leader waveform is characterized by subtle, relatively slow (of the order of several hundred nanoseconds) variations in the electric field within the roughly 5 μs preceding the subsequent return stroke. At the bottom in Figure 3a, we show the energetic radiation measured in association with the same dart leader. A short burst (about 2 μs in duration) of relatively weak energetic radiation was recorded immediately prior to the onset of the return stroke. There were no additional deviations from the system noise with the exception of several weak signals detected about 4 μs prior to the return stroke. At the top in Figure 3b, we show a dE/dt waveform of a typical dart-stepped leader preceding a triggered-lightning return stroke. The dart-stepped leader is characterized by pronounced pulses corresponding to individual leader steps occurring at intervals of 1 to 2 μs. The energetic radiation waveform measured from the same dart-stepped leader is shown at bottom in Figure 3b. Here, discrete bursts of energetic radiation were measured in association with most leader-step pulses presented at the top in Figure 3b. Note that the pulses of energetic radiation are not exactly time aligned with the above dE/dt leader-step pulses because the dE/dt measurement colocated with the $LaBr_3$ sensor saturated during this event, forcing us to plot the output of a different antenna, and hence, introducing propagation path length differences. Finally, at the top in Figure 3c, we show a dE/dt waveform from a "chaotic" dart leader. The "chaotic" dart leader demonstrates the same subtle electric field variations within the 5 μs preceding the return stroke as does the typical dart leader shown at the top in Figure 3a. In addition, however, superimposed on the slower electric field variations is a relatively continuous series of very narrow (of the order of tens of nanoseconds) pulses, frequently with amplitudes

Table 1. General Information on Four "Chaotic" Dart Leaders Recorded Between June and August 2010

Date	Shot Number	GPS Time (UT)	Stroke Order	Peak Current (kA)	Launching Configuration
06/21/2010	UF 10–13	20:09:37.357362	1	43.1	LF2
07/15/2010	UF 10–20	17:28:25.235689	1	17.1	LF1
07/15/2010	UF 10–21	17:35:06.232322	1	22.2	LF1
08/13/2010	UF 10–24	19:44:35.214196	3	28.3	LF1

comparable to the pulses recorded in association with dart-stepped leader dE/dt steps shown in Figure 3b. At the bottom in Figure 3c, we show the energetic radiation measured from the "chaotic" dart leader. A relatively continuous burst of energetic radiation was recorded beginning at about $t = -8$ μs and continuing to the return stroke. The "pileup" characteristic shown is a result of energetic photons arriving at the detector at shorter intervals than the single photon response pulse width (shown in Figure 2 to be about 184 ns) and is not necessarily indicative of the detection of more energetic photons.

[12] From the dE/dt and energetic radiation waveforms presented in Figure 3, it is clear that the electromagnetic emission of the "chaotic" dart leader is distinctly different from that of the typical dart and dart-stepped leaders. "Chaotic" dart leaders exhibit large, high-frequency irregular variations in the electric field immediately prior to the return stroke that are not observed from typical dart leaders. The characteristics of these pulses are also generally dissimilar from dart-stepped leader pulses and occur nearly continuously, as opposed to discretely. In some cases, the distinction between "chaotic" dart leaders and dart leaders is less obvious. Some dart leaders exhibit very pronounced slower background field changes within 10 μs of the return stroke similar to "chaotic" dart leaders, but they do not exhibit a significant series of superimposed high-frequency pulses. As suggested by *Bailey and Willett* [1989] and *Lan et al.* [2011], there may be a continuum of characteristics between the observed electric field emissions of "chaotic" dart leaders and ordinary dart leaders, in part, because of the system noise level, system sensitivity and frequency response, and measurement location. A more clearly defined metric than the characteristics of the dE/dt used previously for differentiating between the "chaotic" dart leader and dart leader processes is

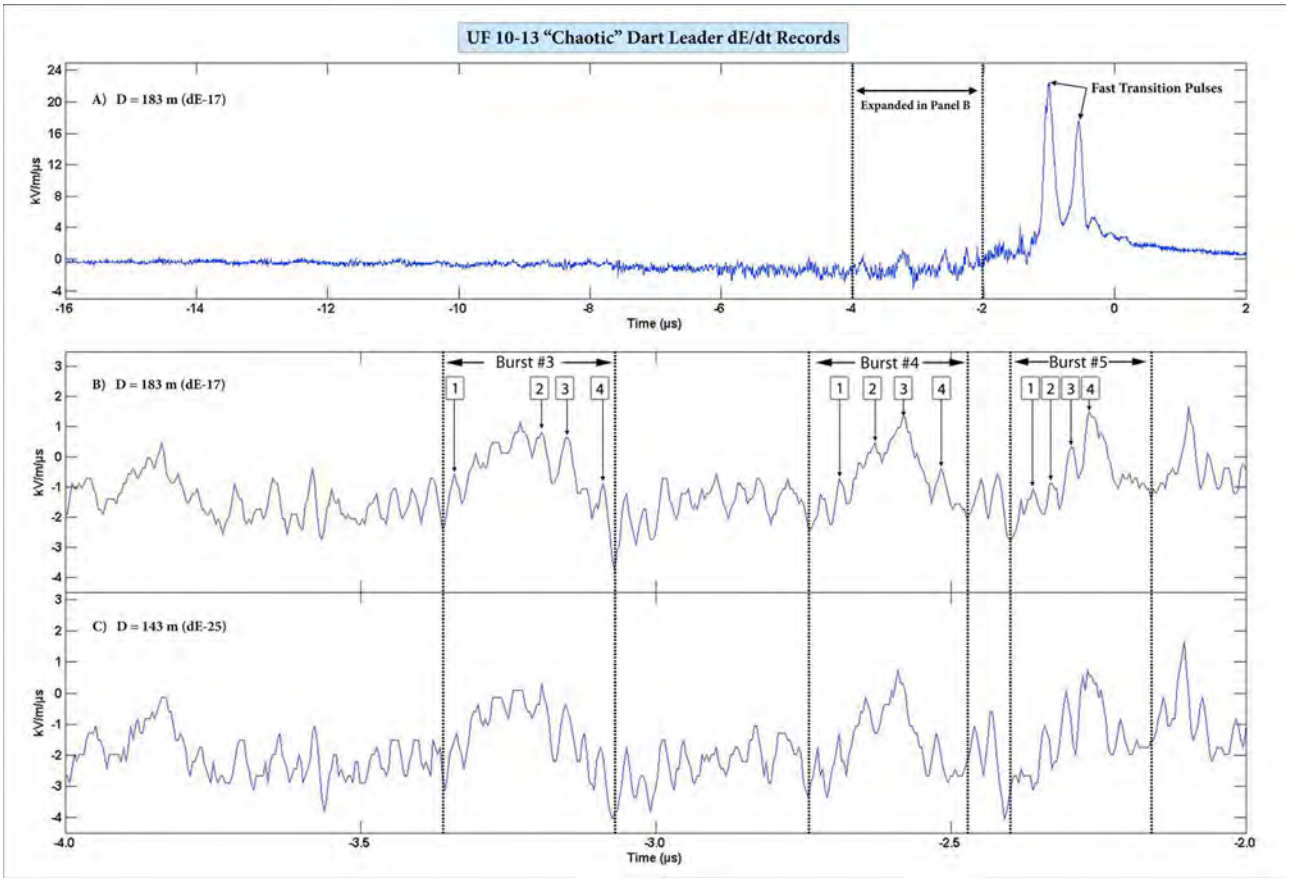

Figure 4. (a) An 18 μs dE/dt record of the "chaotic" dart leader on 21 June 2010, measured 183 m from the lightning channel base. (b) A 2 μs section of the waveform in Figure 4a with three bursts annotated along with sequentially numbered TOA-located pulses in each respective burst. (c) A 2 μs dE/dt waveform measured 143 m from the lightning channel base corresponding to the same time window as Figure 4b.

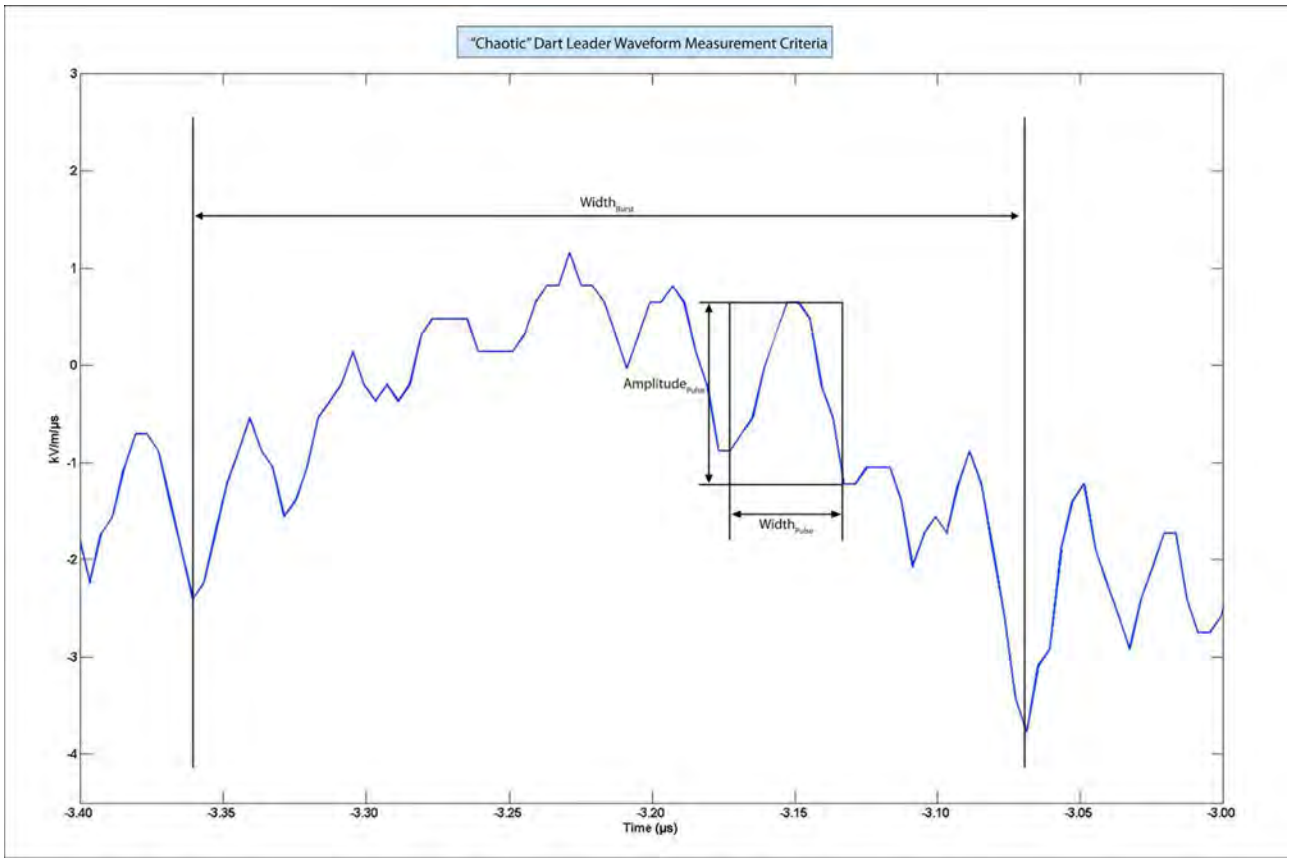

Figure 5. Measurement criteria for burst width, pulse width, and pulse amplitude.

apparently the intense emission of energetic radiation by the "chaotic" dart leader. As shown in Figure 3, the energetic radiation emitted from the "chaotic" dart leader is more continuous and longer in duration than the typical emission from dart leaders and is also dissimilar from the discrete bursts of energetic radiation emitted in association with dart-stepped leader steps.

4. Data and Analysis

[13] A total of four "chaotic" dart leaders were observed between June and August of 2010. General information for each "chaotic" dart leader is shown in Table 1. Shot designations are given in the form "UF 10-XX" where "XX" denotes the shot number of the calendar year. The first event recorded was triggered to the LF2 configuration while the remaining three events were triggered to the LF1 configuration. The first three "chaotic" dart leaders preceded the first return stroke following the explosion of the triggering wire. The final event preceded the third return stroke in a flash that had nine return strokes. The peak return stroke currents measured at the channel base for these events ranged from 17.1 to 43.1 kA, all larger than typical triggered-lightning return stroke peak currents of 10 to 15 kA [e.g., *Rakov and Uman*, 2003]. The electric field derivative and energetic radiation emissions of two "chaotic" dart leaders, events UF 10–13 and UF 10–24, will be analyzed in detail in sections 4.1 and 4.2, respectively. In section 4.3, high-speed video images of two "chaotic" dart leaders triggered to the LF1 configuration will be presented and analyzed.

4.1. UF 10–13

[14] Flash UF 10–13 with one return stroke was triggered to the LF2 launching configuration at 20:09:37.357362 (UT) on 21 June 2010. The measured peak return stroke current was 43.1 kA. An 18 μs plot of the dE/dt waveform measured at station 17, located 183 m from the lightning channel base, is shown in Figure 4a. The pronounced "chaotic" emission is recorded beginning at about time $t = -7.0$ μs in the plot, about 6.0 μs prior to the onset of the return stroke. There were a total of seven slowly varying field changes that we term "bursts." The seven bursts ranged in width from 144 to 384 ns with an average of 261 ns. Burst width measurement was to some extent subjective. Superimposed on each burst were a series of narrow pulses. Shown in Figure 4b, is a 2 μs window of the waveform of Figure 4a bounded by the vertical dotted lines. The amplitude scale in Figure 4b has been reduced to better show the fine structure of the waveform. There are three bursts annotated in Figure 4b by vertical dotted lines, the third, fourth, and fifth bursts measured during the event. Burst 3 had a total width, as shown by the vertical lines, of 292 ns with a total of eight superimposed pulses, burst 4 had total width of 264 ns with seven superimposed pulses, and burst 5 had total width of 240 ns with six superimposed pulses. For each of the three bursts, we have further annotated four individual pulses that are numbered sequentially with increasing time. Shown in Figure 4c

Table 2. Calculated Three Dimensional TOA Locations, Emission Times, Velocities Between Successive Located Pulses, and Associated Errors for Individual Pulses Occurring During Three Bursts for Event UF 10–13 on 21 June 2010, Derived From Measurement of the Peak dE/dt With 4 ns Accuracy

	Pulse Number	x (m)	y (m)	z (m)	t (μs)	$\Delta p/\Delta t$ (10^8 m/s)	Δx (m)	Δy (m)	Δz (m)
Burst 3	1	301.3	447.3	111.0	−4.057	-	0.25	0.63	1.35
	2	301.2	447.9	96.3	−3.895	1.87	0.16	0.23	0.49
	3	307.0	456.4	87.5	−3.823	2.82	0.01	0.02	0.06
	4	308.3	447.3	88.7	−3.790	-	1.84	2.19	5.24
Burst 4	1	299.2	454.7	95.0	−3.391	-	0.04	0.09	0.20
	2	298.5	447.5	61.7	−3.289	7.64	0.01	0.03	0.11
	3	298.5	453.6	80.5	−3.263	1.53	0.01	0.01	0.02
	4	302.0	449.1	69.6	−3.182	-	0.02	0.04	0.19
Burst 5	1	302.9	450.1	65.6	−3.022	15.40	0.70	0.71	2.91
	2	301.6	453.0	79.4	−3.013	2.95	0.02	0.02	0.09
	3	300.2	451.6	63.8	−2.960	4.28	0.03	0.04	0.30
	4	299.7	451.2	74.2	−2.936	-	0.04	0.07	0.11

is a second dE/dt waveform measured 143 m from the lightning channel base at station 25, corresponding to the time region shown in Figure 4b. The purpose of this plot is to show the correlation of the burst and pulse waveform features across multiple channels. A similar aligning process is used for all ten dE/dt channels when TOA calculations are performed.

[15] There were a total of 73 pulses analyzed for shape and amplitude. Measurement criteria for burst width, pulse width, and pulse amplitude are illustrated in Figure 5. Pulses ranged in full width from 12 to 68 ns and in amplitude above the burst level from 0.5 to 3.6 kV/m/μs (at a distance of 183 m). The average full pulse width was 37 ns with standard deviation of 11 ns, and the average pulse amplitude was 1.6 kV/m/μs with standard deviation of 0.5 kV/m/μs. The full width of the pulses were measured as opposed to the full width at half-maximum because the sampling frequency was typically insufficient to establish an accurate half-maximum amplitude. Pulse amplitude was measured from the pulse peak to the lesser amplitude of the two pulse endpoints. We estimate that both the true pulse width and amplitude could differ from our somewhat subjectively measured values,

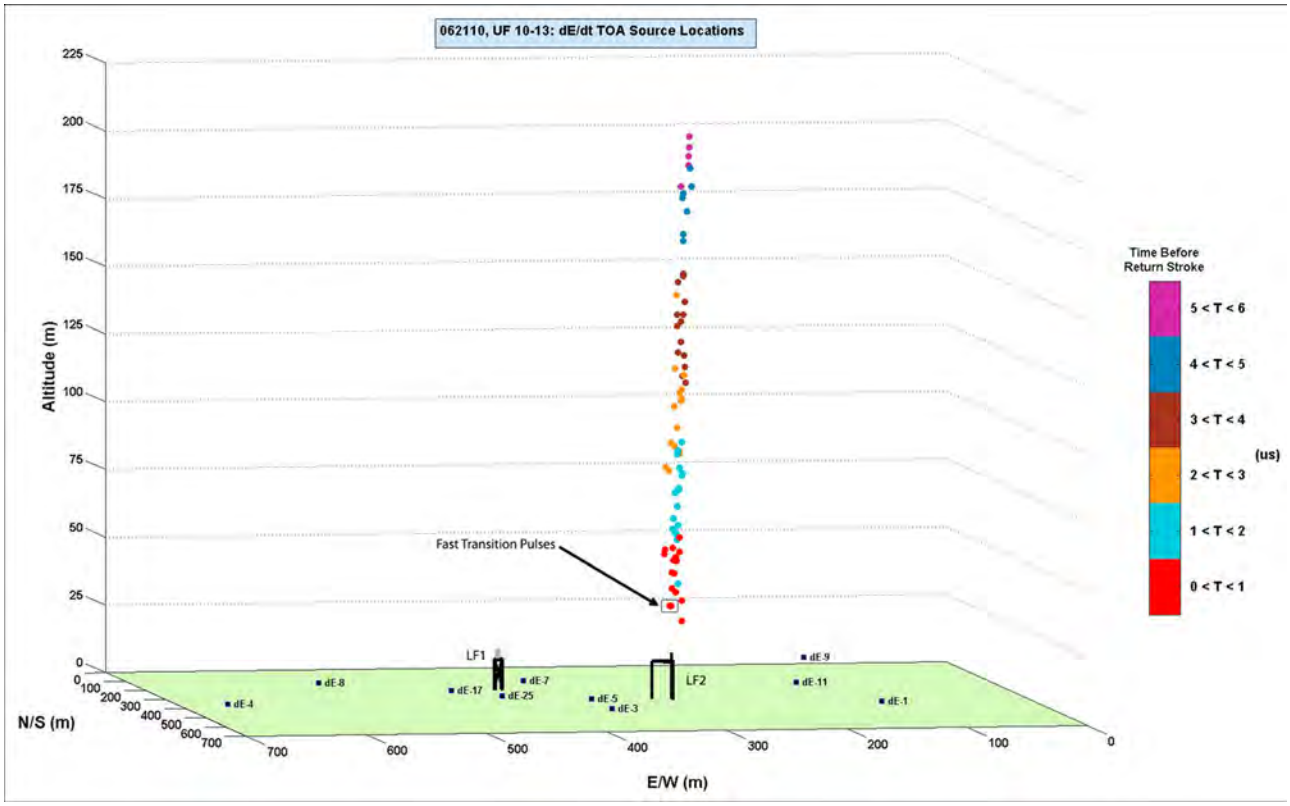

Figure 6. TOA source locations for 75 pulses located during the "chaotic" dart leader on 21 June 2010. Points are color-coded based on calculated emission time relative to the return stroke. The locations of the 10 dE/dt sensors are shown.

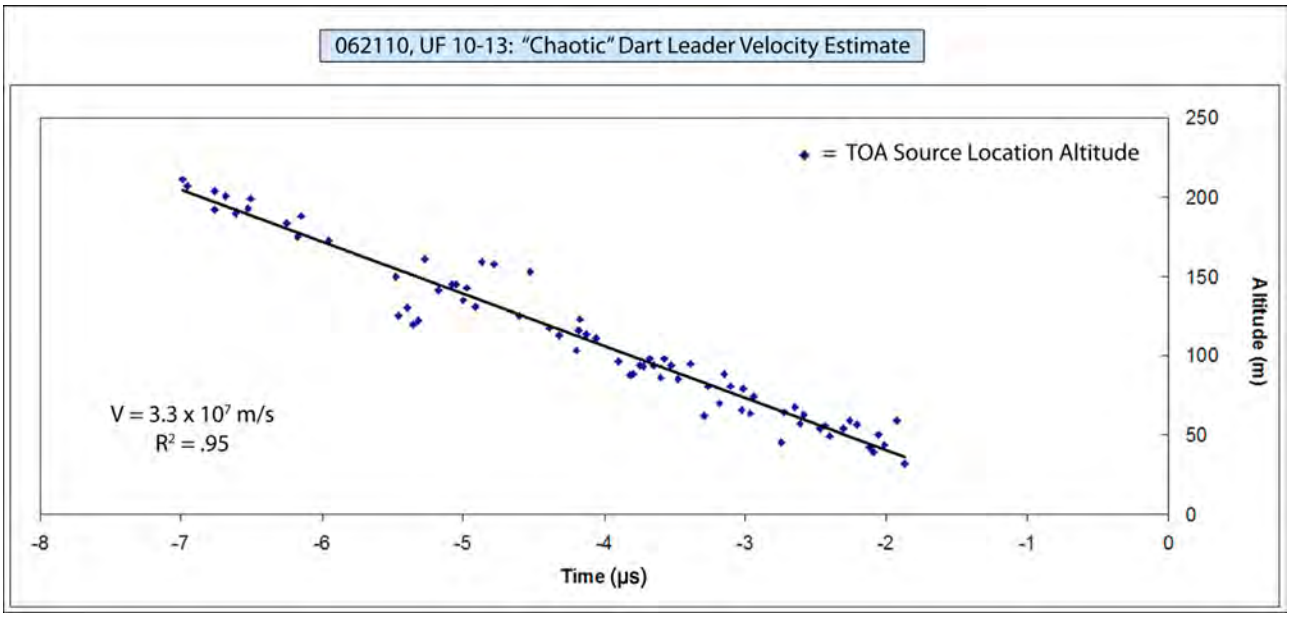

Figure 7. Best fit estimate for vertical velocity of the "chaotic" dart leader on 21 June 2010 using TOA source locations.

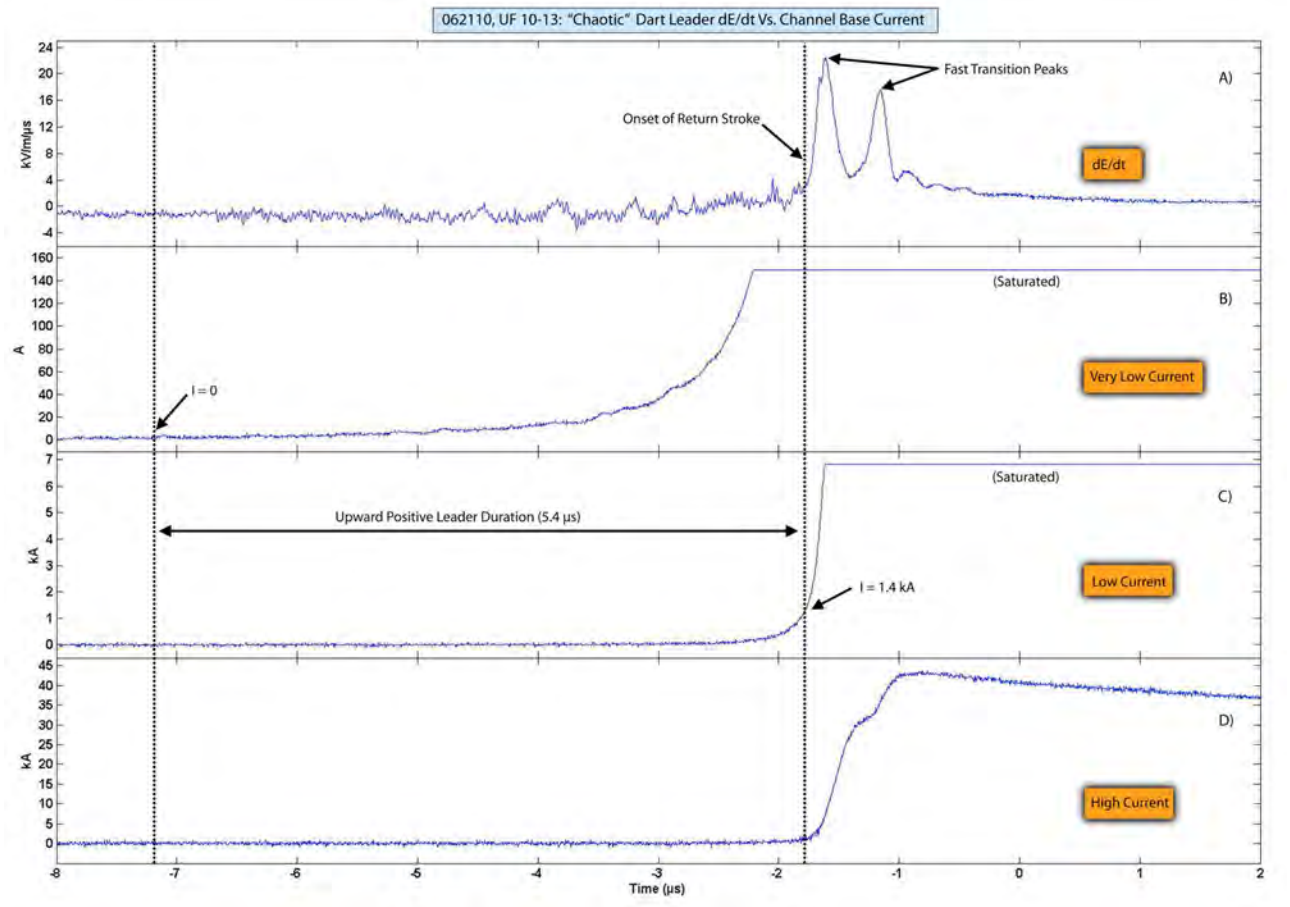

Figure 8. (a) A dE/dt waveform measured 183 m from the lightning channel base. (b, c, d) Channel base current waveforms of three different sensitivities. The time of the initial current rise from zero and the time of the return stroke onset with corresponding current amplitude are labeled with dotted vertical lines. The duration of the upward positive leader is measured to be 5.4 μs.

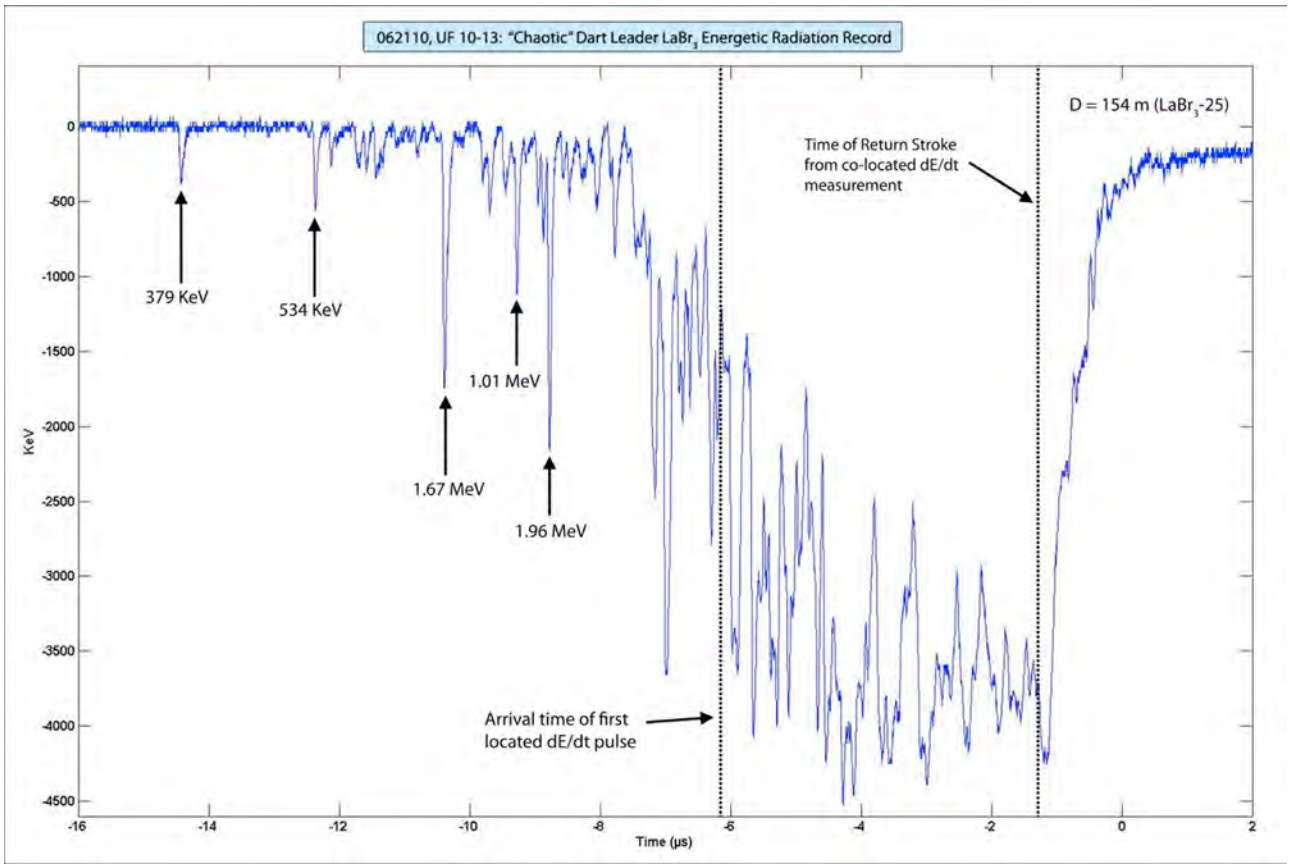

Figure 9. $LaBr_3$ energetic radiation record for the "chaotic" dart leader on 21 June 2010 measured a distance of 154 m from the lightning channel base. The time of the return stroke and the arrival time of the first located dE/dt pulse are marked by dotted vertical lines. Five detected single photon events are labeled with their respective energies.

width by 30%–50% and amplitude by as much as a factor of 2. In addition, it is possible the pulses are, in fact, narrower than observed but are bandwidth limited by the antenna and fiber-optic link.

[16] The three-dimensional source locations (x, y, z) and associated location uncertainties (Δx, Δy, Δz), along with the emission times (t) for the 12 located pulses determined using the TOA technique described in section 2 are given in Table 2. Also provided in Table 2 are the calculated velocities between subsequent source locations ($\Delta p/\Delta t$). Calculated velocities are given only for those cases in which successive pulses in the record were located. Considering the typically straight and vertical geometry of a triggered-lightning channel at low altitude, it is not surprising that the lateral (x, y) source location estimates for the located pulses in all three bursts fall within a plane of dimensions roughly 10 m square. The estimated altitude source locations, however, tend to vary fairly significantly among the pulses within a given burst. For burst 3, the estimated altitude source locations for pulses 1–3 decrease linearly. In burst 4, the estimated altitude source locations for each locatable pulse appear to "bounce" up and down for each subsequent pulse, differing by as much as 33 m between adjacent pulses. Interestingly, the calculated velocities between pulse 1 and pulse 2 and between pulse 2 and pulse 3 both exceed the speed of light. The most likely explanation for this fact is that high-frequency emission is being radiated from multiple (perhaps many) points within a few tens of meters of the leader tip, nearly simultaneously. The four consecutive pulses located within burst 5 also have altitude source location estimates that bounce up and down for each subsequent pulse, varying by up to 15 m between adjacent pulses. Once again, the calculated velocities between all three sets of subsequent pulses approach or exceed the speed of light.

[17] There were a total of 73 pulses located within the 6 μs prior to the return stroke, ranging from a maximum altitude of about 211 m to a minimum altitude of about 32 m. The top of the intercepting rod in the LF2 launching configuration was located at an altitude of about 18 m with respect to the local coordinate system origin (about 14 m above local ground level). In Figure 6, three-dimensional source locations for all located pulses are plotted. The data points are color-coded in 1 μs intervals based on the emission time relative to the return stroke. Two additional data points in a small black box at the bottom of the channel correspond to the source locations for the two fast-transition peaks associated with the onset of the return stroke (two large pulses annotated on Figure 4a, peaking at approximately $t = -1.0$ μs and $t = -0.5$ μs respectively), both at altitudes of about 37 m and at the junction point(s) of the downward and upward connecting leaders from the launch facility [e.g., *Jerauld et al.*, 2007; *Howard et al.*, 2010]. The spatial locations

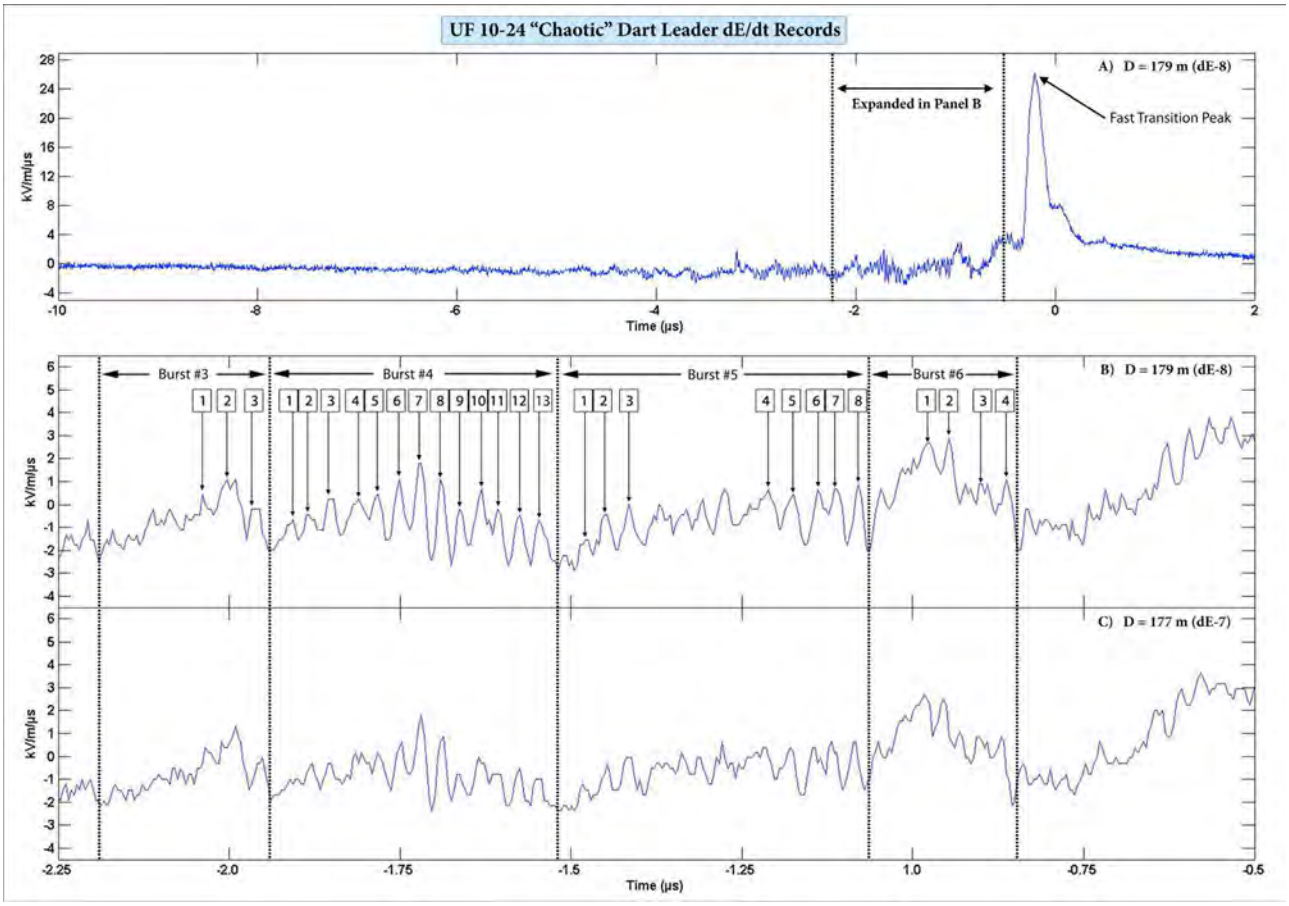

Figure 10. (a) A 12 μs dE/dt record of the "chaotic" dart leader on 13 August 2010, measured 179 m from the lightning channel base. (b) A 1.75 μs section of the waveform in Figure 10a, with four bursts annotated along with sequentially numbered TOA-located pulses in each respective burst. (c) A 1.75 μs dE/dt waveform measured 177 m from the lightning channel base corresponding to the same time window as Figure 10b.

of the ten dE/dt sensors are also plotted in Figure 6 for reference.

[18] The vertical velocity of the "chaotic" dart leader was estimated by fitting a line to a scatterplot of the altitude source locations versus emission time for the 73 pulses located prior to the return stroke. The plot and corresponding line of best fit are shown in Figure 7. The estimated vertical velocity was 3.3×10^7 m/s with a correlation coefficient of 0.95.

[19] In Figure 8a, a dE/dt waveform is plotted, which was measured 183 m from the lightning channel base. In addition, three channel base current waveforms are shown at different sensitivities in Figures 8b–8d. The channel base current waveforms were obtained from three different measurements with sensitivities to record peak currents to about 150 A for the very low current, about 6.7 kA for the low current, and about 55 kA for the high current. Cabling delays have been removed from all waveforms. In addition, the propagation delay from the spatial location of the first fast-transition pulse to the dE/dt sensor has also been removed from the waveform in Figure 8a. Finally, the delay to the CVR of the downward-moving return stroke current wave initiated at the spatial location of the fast-transition pulse has been removed from all the current waveforms, assuming a current propagation velocity of 1.1×10^8 m/s. In Figure 8b, the channel base current begins to increase from the system noise level (current is assumed to be zero at this point) at about $t = -7.2$ μs. This point is annotated by a dotted vertical line. The current increases relatively slowly over the next 4 μs to a level of about 28 A, after which the current increases more rapidly over the next 1.4 μs. At $t = -1.8$ μs, the onset of return stroke occurs in the dE/dt record plotted in Figure 8a. The relatively slow and smooth current rise over the time span of about 5.4 μs likely indicates the initiation of an upward positive leader [e.g., *Lalande et al.*, 1998]. The current at this time is annotated with a dotted vertical line and is at a level of about 1.4 kA, apparently the peak value of the upward leader current. If we assume that the two fast-transition pulses, which we located at an altitude of about 37 m, originate with the connections of the upward and downward leaders, the upward positive leader would have needed to propagate at an average velocity of about 3.7×10^6 m/s to traverse the 20 m distance between the top of the intercepting rod and the spatial location of the fast-transition pulses.

[20] The "chaotic" dart leader of UF 10–13 was an intense emitter of energetic radiation. In Figure 9, we have plotted an 18 μs record of the energetic radiation measured by a

Table 3. Calculated Three Dimensional TOA Locations, Emission Times, Velocities Between Successive Located Pulses, and Associated Errors for Individual Pulses Occurring During Four Bursts for Event UF 10–24 on 13 August 2010, Derived From Measurement of the Peak dE/dt With 4 ns Accuracy

	Pulse Number	x (m)	y (m)	z (m)	t (μs)	$\Delta p/\Delta t$ (10^8 m/s)	Δx (m)	Δy (m)	Δz (m)
Burst 3	1	445.3	419.5	106.1	−2.733	1.31	0.01	0.02	0.06
	2	445.7	421.7	100.6	−2.687	-	0.01	0.01	0.02
	3	449.9	422.9	103.6	−2.658	3.91	0.43	0.35	1.28
Burst 4	1	453.3	424.9	110.4	−2.638	3.38	0.84	0.30	1.17
	2	440.9	424.6	86.6	−2.559	5.17	0.02	0.02	0.08
	3	445.4	417.7	96.9	−2.533	0.91	0.12	0.13	0.38
	4	444.1	417.6	92.7	−2.486	1.30	0.10	0.11	0.32
	5	446.9	419.2	93.0	−2.461	1.08	0.40	0.55	1.76
	6	445.4	419.2	88.9	−2.421	0.28	0.18	0.31	0.92
	7	444.6	419.6	88.9	−2.391	1.71	0.18	0.25	0.81
	8	446.1	420.6	92.4	−2.368	3.45	0.02	0.04	0.11
	9	443.7	419.6	76.6	−2.321	1845	0.09	0.10	0.93
	10	445.7	418.4	103.8	−2.322	-	0.47	0.86	2.34
	11	442.5	418.8	75.6	−2.265	2.60	0.12	0.13	1.25
	12	444.5	419.3	82.5	−2.237	1.43	0.05	0.07	0.23
	13	444.4	416.7	77.8	−2.199	2.67	0.02	0.03	0.13
Burst 5	1	443.4	419.8	89.1	−2.155	-	0.17	0.18	1.55
	2	443.7	419.6	79.0	−2.104	0.42	0.64	0.69	2.94
	3	443.7	418.3	78.6	−2.073	-	0.37	0.49	1.85
	4	442.3	419.3	71.1	−1.865	1.06	0.47	0.28	2.55
	5	443.1	416.7	66.4	−1.814	2.82	1.49	1.83	8.53
	6	443.1	417.7	54.3	−1.771	19.0	0.03	0.03	0.28
	7	444.4	417.5	71.9	−1.762	0.71	0.37	0.42	1.44
	8	444.5	419.2	70.1	−1.727	-	0.28	0.31	1.20
Burst 6	1	444.4	416.5	49.8	−1.602	2.80	0.06	0.10	0.44
	2	443.3	416.5	56.4	−1.578	-	0.17	0.20	1.07
	3	446.4	418.9	57.4	−1.533	-	1.10	1.19	5.40
	4	444.0	415.0	34.6	−1.473	-	0.03	0.04	0.31

$LaBr_3$/PMT detector located 154 m from the lightning channel base. A relatively continuous burst of energetic radiation pulses begins at about $t = -12.5$ μs in the plot, about 11 μs prior to the return stroke. For the next 5 μs time period, ending at about $t = -7.5$ μs, the emission is often recorded with enough time between incident photons to allow the detector output to decay back near the zero level prior to the arrival of the next photon(s). Many of the pulses recorded during this time period have widths of the order of 200 ns, suggesting, from Figure 2, that the detector recorded single photons. A fit of the detector response to the apparently single photon events reveals that most of the detected photons have energies between several hundred keV to about 2 MeV. The energies for five single photon events were calculated and are shown in Figure 9 beneath the vertical arrows. If we assume that the downward leader propagated with relatively constant velocity at low altitude, we can use the velocity estimate calculated from the dE/dt TOA locations in Figure 6 to estimate the height of the leader at the beginning of the continuous burst of energetic radiation at $t = 12.5$ μs. This calculation yields an altitude of 395 m, about 184 m higher in altitude than the highest located dE/dt pulse. After a time $t = -7.5$ μs in the plot, the detected photons arrive with interpulse intervals too short to allow the detector to decay prior to the arrival of the next photon. This pronounced "pileup" effect extends through the time of the return stroke, which is labeled and annotated in Figure 9 by a black dotted line. The time of the return stroke was determined by aligning the waveform from the colocated dE/dt sensor with the $LaBr_3$/PMT detector waveform, accounting for signal transit delays over coaxial and fiber-optic cables. To understand why the single, higher-energy photons were detected preceding the pileup of photons, the measured energies of which are undetermined, we performed Monte Carlo simulations starting with an initially spatially localized region of energetic electrons at several heights above ground. The results of the simulation show that, for distant sources that occur a relatively long time before the return stroke, the single, higher-energy photons arrive at the detectors without appreciable Compton scattering, while for closer sources occurring just before the return stroke, many photons from the assumed source arrive at the detector closely spaced in time. Interestingly, pulses of energetic radiation were detected for over a microsecond after the time of the return stroke. It is generally thought that energetic radiation is only associated with the leader processes, and most records do indeed show the radiation ending at the start of the return stroke.

4.2. UF 10–24

[21] Flash UF 10–24 with nine return strokes was triggered to the LF1 launching configuration on 13 August 2010 at 19:44:35.013453 UT. The first two strokes of this flash had peak currents of 11.2 kA and 10.2 kA, respectively, and both were preceded by typical dart leaders. The third stroke had a peak current of 28.3 kA and was preceded by a "chaotic" dart leader. The fourth, sixth, and eighth strokes of the event were preceded by dart-stepped leaders, and the fifth, seventh, and ninth return strokes were preceded by normal dart leaders. Of the four "chaotic" dart leaders

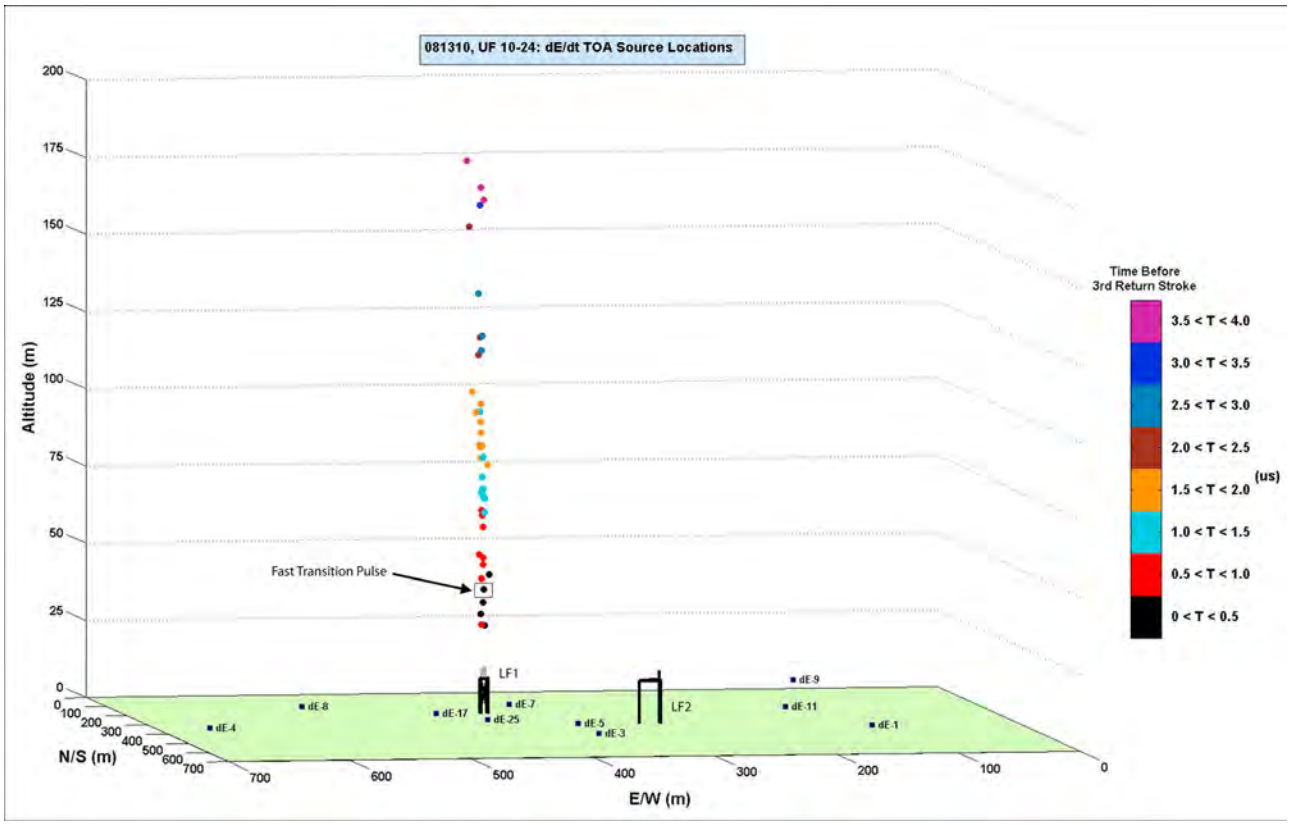

Figure 11. TOA source location estimates for 45 pulses located during the "chaotic" dart leader on 13 August 2010. Points are color-coded based on calculated emission time relative to the return stroke. The locations of the 10 dE/dt sensors are shown.

recorded during summer 2010, this was the only one that did not precede the first return stroke. Similar to the other three events, this "chaotic" dart leader preceded the stroke with the largest peak current of the flash.

[22] In Figure 10a, we show a 12 μs dE/dt record of the "chaotic" dart leader measured at station 8, a distance of 179 m from the lightning channel base. The pronounced "chaotic" emission is recorded beginning at about $t = -6.0$ μs and continues through the time of the return stroke at about $t = -0.3$ μs. Similar to the event discussed in section 4.1, the "chaotic" emission during this event can be generally characterized as relatively continuous series of narrow (tens of nanoseconds) pulses superimposed on slower (hundreds of nanoseconds) background field changes, which we termed "bursts." There were a total of seven bursts recorded during this event. We have annotated four bursts in Figure 10b, the third, fourth, fifth, and sixth bursts measured during this event. The temporal extent of each burst is marked by vertical dotted lines. Burst 3 had a total width of 252 ns with ten superimposed pulses; burst 4 had a total width of 416 ns with 13 superimposed pulses; burst 5 had a total width of 456 ns with 15 superimposed pulses; and burst 6 had a total width of 224 with seven superimposed pulses. For each burst, we have further annotated individual pulses with integers increasing in time. Figure 10c shows a second dE/dt waveform measured 177 m from the lightning channel base at station 7, corresponding to the time region shown in Figure 10b. Again, the purpose of this plot is to show the correlation of the burst and pulse waveform features for this event across multiple channels.

[23] There were a total of 45 individual pulses analyzed for waveshape and amplitude. These pulses ranged in width from 24 to 48 ns and ranged in amplitude from 0.7 to 4.2 kV/m/μs (at a distance of 179 m). The average pulse width was about 32 ns with standard deviation of about 6 ns and the average pulse amplitude was about 2.0 kV/m/μs with standard deviation of 0.7 kV/m/μs. The three-dimensional source locations, associated location uncertainties, emission times, and calculated velocities between subsequent source locations for these pulses are given in Table 3.

[24] Similar to event UF 10–13, the lateral source location estimates for all of the located pulses during the four bursts annotated in Figure 10 occur within a spatial region of about 10 m^2. In burst 3, three of the final four pulses of the burst were located. The altitude coordinates of the three source locations covered a spatial region of about 6 m and tended to bounce up and down with increasing time over a time span of about 75 ns. There were a total of 13 pulses superimposed on burst 4, all of which were located. The first pulse of the burst occurred at an altitude of 110 m, followed over the next 191 ns by seven subsequent pulses all with altitude coordinates varying from 88 to 96 m. There was no apparent spatial pattern to the source locations of these seven pulses. The ninth pulse of the burst was located at an altitude of 76 m followed by the tenth pulse at 103 m. Interestingly, the emission time of the tenth pulse was calculated to be a

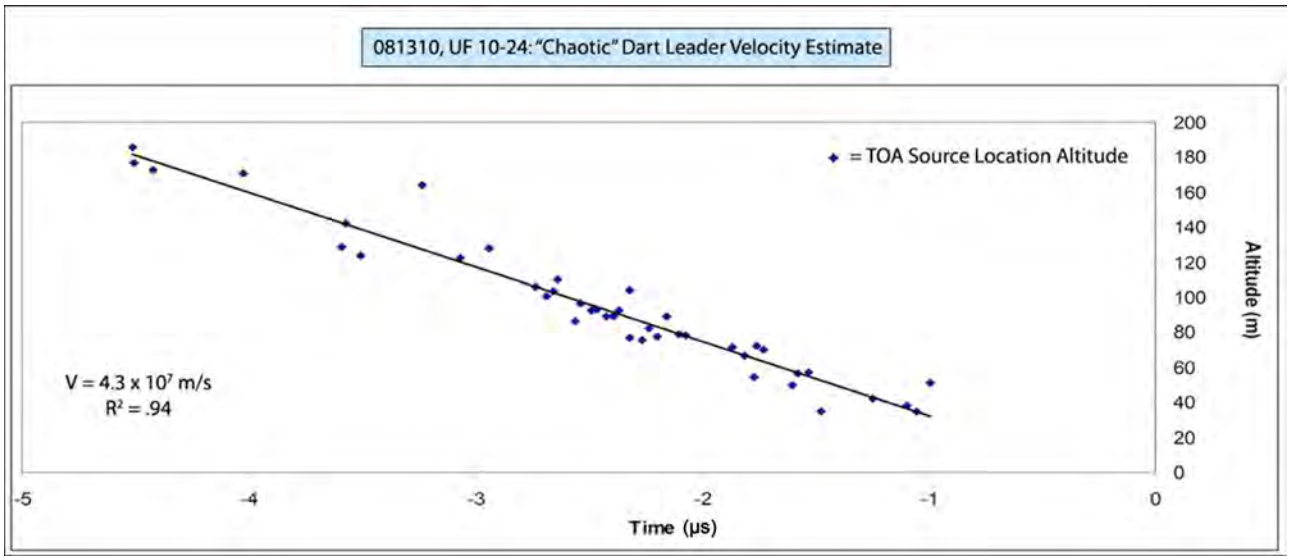

Figure 12. Best fit estimate for vertical velocity of the "chaotic" dart leader on 13 August 2010 using TOA source locations.

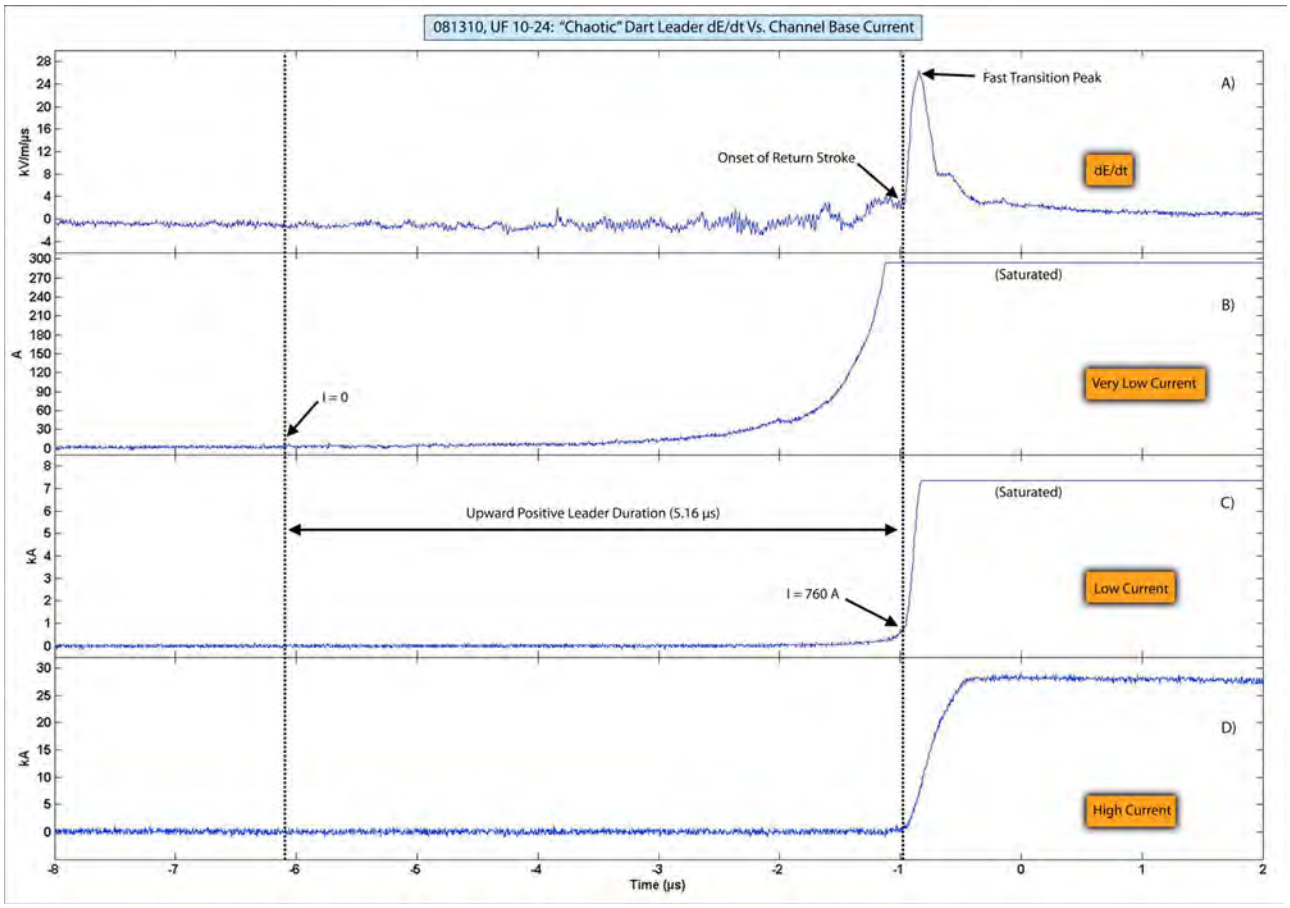

Figure 13. (a) A dE/dt waveform measured 179 m from the lightning channel base. (b, c, d) Channel base current waveforms of three different sensitivities. The time of the initial current rise from zero and the time of the return stroke onset with corresponding current amplitude are labeled with dotted vertical lines. The duration of the upward positive leader is measured to be 5.16 μs.

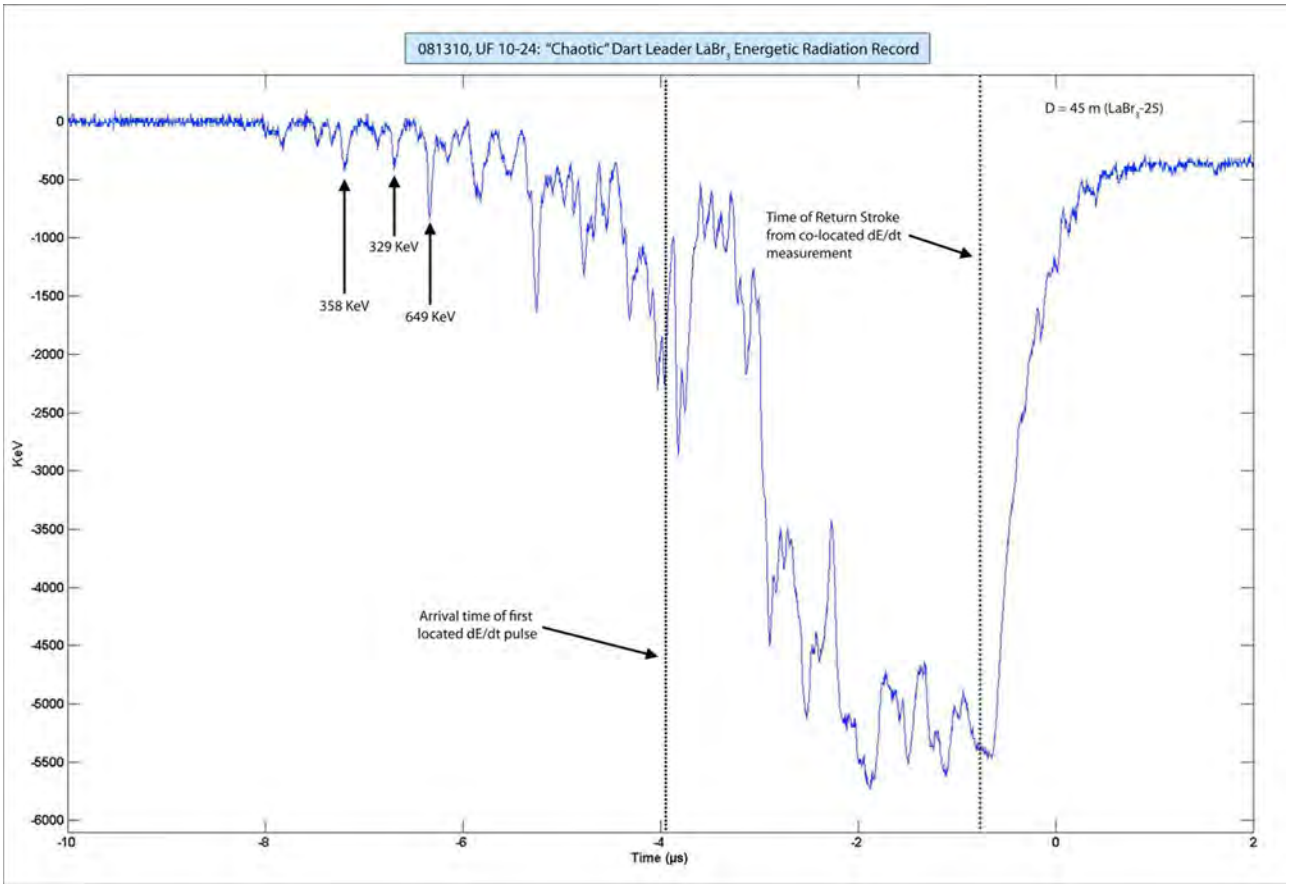

Figure 14. $LaBr_3$ energetic radiation record for the "chaotic" dart leader on 13 August 2010 measured a distance of 45 m from the lightning channel base. The time of the return stroke and the arrival time of the first located dE/dt pulse are marked by dotted vertical lines. Three detected single photon events are labeled with their respective energies.

fraction of a nanosecond prior to the ninth pulse, but occurred about 27 m higher in altitude. The final three pulses of the burst fluctuated in altitude from about 75 to 82 m over a time span of about 65 ns and also tended to bounce up and down with increasing time. There were a total of eight located pulses in burst 5. The first three located pulses were consecutive at the beginning of the burst and decreased in altitude from 89 to 78 m over a time span of about 82 ns. The next six pulses in the record increasing in time were not locatable. The final five pulses in the record were located. Pulses 4 through 6 decrease in altitude from 71 to 54 m over a time period of about 94 ns. Pulse 7 was emitted only 10 ns later in time than pulse 6, but at an altitude of almost 72 m, a distance of about 18 m above pulse 6. The final pulse in the burst was located with similar altitude to pulse 7. There were four pulses successfully located within burst 6. The first two pronounced pulses in the burst were not locatable. Pulse 1 was located at an altitude of about 50 m. Pulse 2 and pulse 3 were separated in emission time by about 45 ns but occurred within a meter of each other in altitude. Pulse 4 was the final pulse in the burst and was located at an altitude of 34 m, separated in altitude from pulse 3 by over 23 m and in emission time by 60 ns. Similar to the results presented for event UF 10–13 in section 4.1, in the four bursts discussed in detail above, there were six cases in which the calculated velocities between subsequent source locations exceeded the speed of light and an additional four cases where the calculated velocities between subsequent source locations approached the speed of light.

[25] There were a total of 45 pulses located during this "chaotic" dart leader within the four microseconds prior to the return stroke. In Figure 11, we have plotted three-dimensional source locations for all 45 located pulses. The located pulses ranged in altitude from a maximum of about 185 m to a minimum of about 34 m. The top of the rocket tubes in the LF1 launching configuration are at an altitude of about 20.6 m referenced to the origin of the local coordinate system (about 14 m above local ground). The data points are color-coded based on the emission time relative to the return stroke in 500 ns intervals. We have annotated one additional data point by a small black box near the bottom of the channel corresponding to the source location of the fast-transition peak (the large pulse annotated on Figure 10a, peaking at approximately $t = -0.2$ μs), at an altitude of about 46 m.

[26] The vertical velocity of this "chaotic" dart leader was estimated by fitting a line to a scatterplot of the altitude source locations versus emission time for the 45 pulses

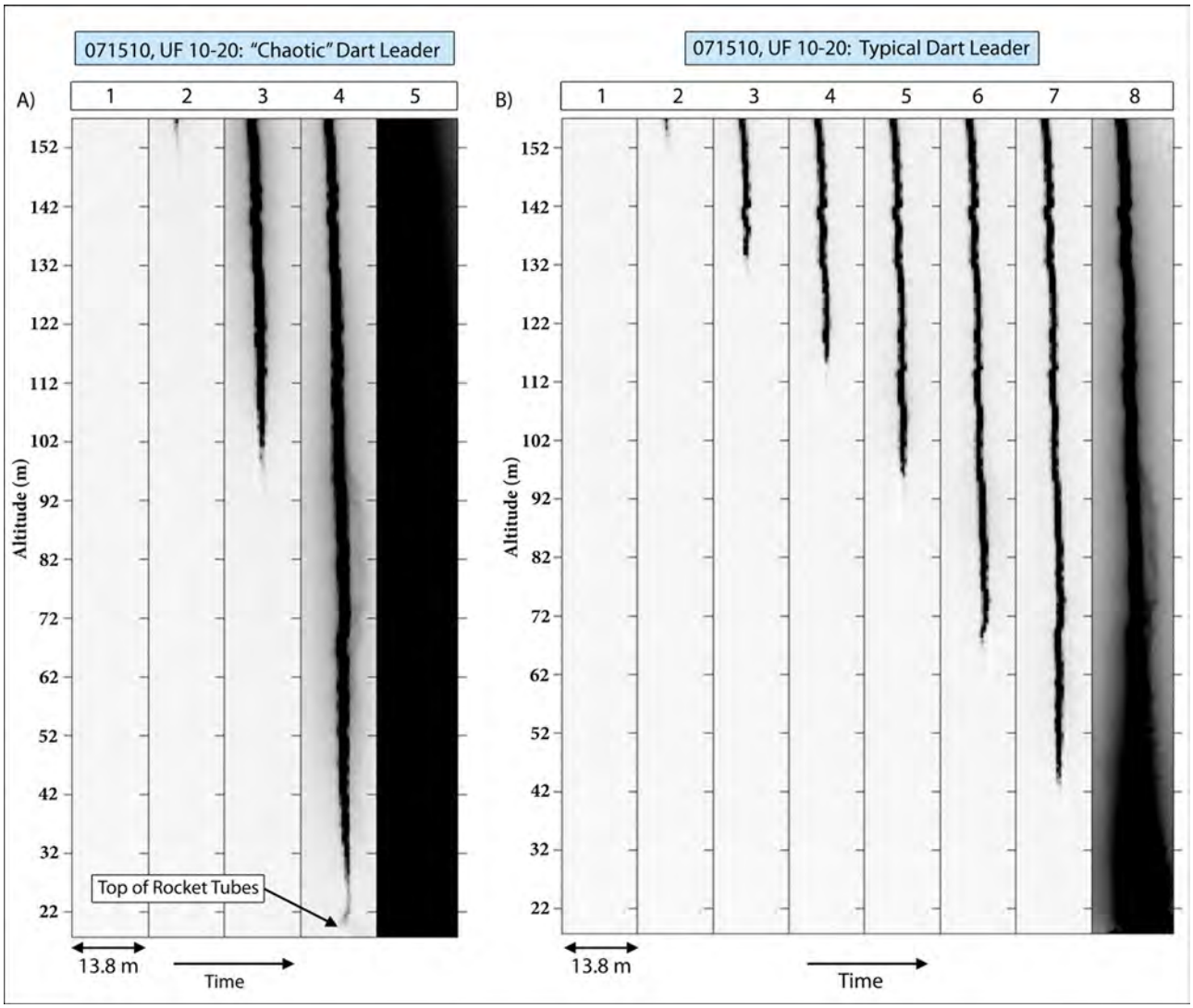

Figure 15. (a) Comparison of high-speed video images recorded during a "chaotic" dart leader and (b) a typical dart leader during the same triggered-lightning discharge event UF 10–20 on 15 July 2010. Each frame corresponds to a 3.33 μs exposure time. Altitudes are given with respect to the local coordinate system origin.

located prior to the return stroke, as shown in Figure 12. The estimated vertical velocity was 4.3×10^7 m/s with a correlation coefficient of 0.94.

[27] In Figure 13a, we have plotted a dE/dt waveform measured 179 m from the lightning channel base in addition to three channel base current waveforms in Figures 13b–13d. The channel base current waveforms were obtained with three different sensitivities, to currents of about 290 A for the very low current, about 6.3 kA for the low current, and about 51 kA for the high current. Cabling and propagation delays have been removed using the methods discussed in section 4.1. In Figure 13b, the channel base current increases from the system noise level at about $t = -6.1$ μs in the plot, annotated by the dotted vertical line. Similar to the case presented for event UF 10–13, the current increases slowly over the next 4 μs to a level of about 38 A, followed by a more rapid increase over the next approximately 1.2 μs to the time of the return stroke onset, again marked by a dotted vertical line. The relatively slow and smooth increase in channel base current during the 5.16 μs prior to the return stroke likely indicates the initiation of an upward positive leader, a hypothesis supported by our high-speed video data. The current at the time of the return stroke onset is about 760 A, apparently the peak value of the upward leader current. An upward leader with length of 11.5 m was imaged in a single 3.33 μs frame integration immediately prior to the return stroke. The downward leader was also imaged in the same frame with the bottom of the streamer zone located about 28 m above the upward leader tip. The high-speed video data for this event will be shown and discussed in detail in section 4.3. The single fast-transition pulse for this event was located at an altitude of about 46 m and slightly south of the launcher, a total distance of about 30 m from the top of the rocket tubes in the LF1 launching configuration. Given a duration of 5.16 μs, the upward positive leader would have needed to propagate at an average velocity of

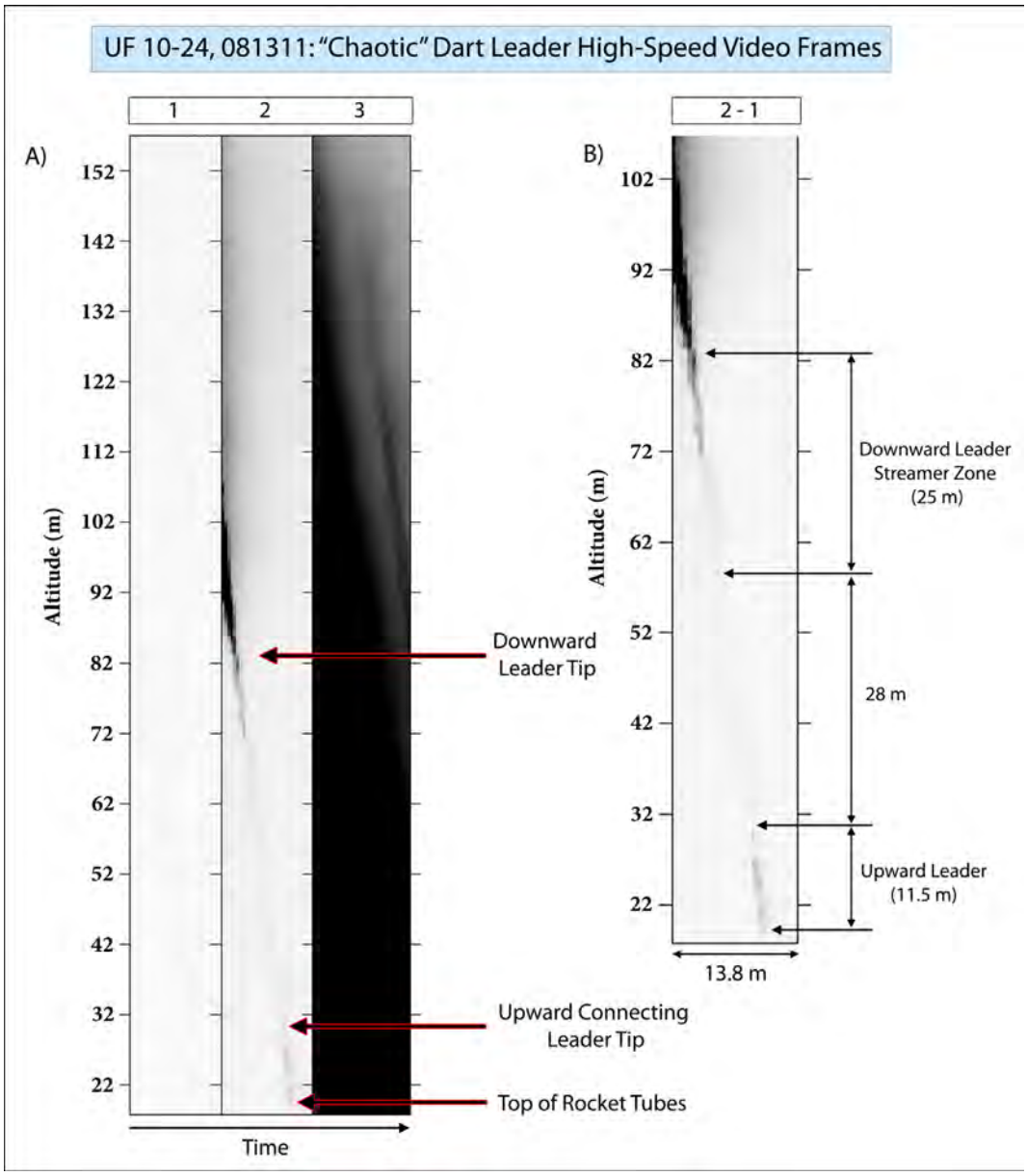

Figure 16. High-speed video images of event UF 10–24 on 13 August 2010. (a) Three consecutive 3.33 μs frames. The downward leader enters the field of view in frame 2. An upward connecting leader is also seen in frame 2. The attachment process and return stroke occur during frame 3. (b) The subtraction of frame 1 from frame 2 with a compressed altitude scale. The lengths of the downward leader's streamer zone and upward leader are annotated. Altitudes are given with respect to the local coordinate system origin.

about 5.8×10^6 m/s in order to traverse the distance between the rocket tubes and the spatial location of the fast-transition pulse.

[28] The "chaotic" dart leader of UF 10–24 was, like all the "chaotic" dart leaders, an intense emitter of energetic radiation. Figure 14 shows a 12 μs record of energetic radiation measured a distance of 45 m from the lightning channel base with a $LaBr_3$/PMT detector. This is the same detector used in the analysis of event UF 10–13 discussed in section 4.1. The beginning of the energetic radiation burst occurs at about $t = -8.0$ μs in the plot. Over the next approximately 2.6 μs, a number of pulses are recorded with widths indicating that the sensor was excited by single photons. For three of these apparently single photon events, a fit of the detector response to the pulses of energetic radiation provides energies ranging from 329 to 649 keV. The three energetic radiation pulses analyzed are annotated in Figure 14 with vertical arrows. From the leader velocity estimate calculated from the dE/dt TOA locations in Figure 11, the extrapolated height of the leader at the beginning of the continuous burst of energetic radiation is at an altitude of about 350 m, about 165 m higher in altitude than the highest located dE/dt pulse. After about $t = -5.4$ μs in the plot, the interpulse intervals from photons incident on the detector are insufficient to allow the sensor to decay. A pronounced pileup effect ensues for the next 6 μs. Similar to event UF

10–13, the energetic radiation appears to continue for about a microsecond after the return stroke, which is labeled and marked with a dotted vertical line in Figure 14. The time of the return stroke is determined using the same method discussed in section 4.1.

4.3. High-Speed Video Images of "Chaotic" Dart Leaders

[29] High-speed video images were obtained for three of the four "chaotic" dart leaders recorded during summer 2010, all except event UF 10–13 on 21 June 2010. The three events were triggered to the LF1 launching configuration, a distance of 430 m from the camera location (Figure 1). The video frame rate was 300 kfps, an exposure time of 3.33 μs. In Figure 15a, we have plotted three consecutive frames of the "chaotic" dart leader that preceded the first return stroke, with peak current of 17.1 kA, of event UF 10–20, triggered on 15 July 2010. In Figure 15b, we have plotted eight consecutive frames of the dart leader preceding the fourth return stroke of the same event. The fourth return stroke had peak current of 11.7 kA and occurred 122 ms after the first return stroke. The purpose of this figure is to illustrate the differences in optical characteristics between a "chaotic" dart leader and a dart leader measured during the same triggered-lightning discharge. For both leaders shown, the images have been inverted, equally contrast enhanced, and the pixel gain (gamma) has been increased by a factor of 2 to better show the lower luminosity features of the leaders. The altitude scales in Figure 15 are referenced to the local coordinate system origin. We see three notable differences: (1) From the images shown, the velocity of the "chaotic" dart leader is estimated to be about 2.0×10^7 m/s, while the dart leader velocity is estimated to be about 6.6×10^6 m/s, a factor of 3 difference; (2) the apparent width of the channel and the apparent surrounding corona region of the "chaotic" dart leader are significantly larger than that of the dart leader; and (3) the length of the streamer zone at the tip of the "chaotic" dart leader is longer than that of the dart leader. We define the beginning of the streamer zone spatially as the pixel beneath the brightly illuminated leader tip (which typically saturates the sensor), where the pixel intensity falls below 75% of the saturation point. Using this criterion, the streamer zones in frames 2, 3, and 4 for the "chaotic" dart leader in Figure 15a are all 8 to 9 m in length, and the streamer zones in frames 2–7 for the typical dart leader in Figure 15b are all 2 to 5 m in length. In frame 4 of Figure 15a, it is unclear whether the lower luminosity section of the channel connecting the brightly illuminated leader tip to the top of the rocket tubes is an elongated streamer zone, an upward leader, or a combination of both. The frame integration ended immediately prior to the onset of the return stroke, which is shown fully saturating the sensor in frame 5.

[30] In Figure 16a, we have plotted three consecutive frames of the "chaotic" dart leader preceding the third return stroke of event UF 10–24. The peak current of the return stroke was 28.3 kA. The electric field derivative and energetic radiation emissions of this event were presented in section 4.2. As a result of the channel tilt to the north, only one frame of the leader phase was captured (frame 2). The images have been inverted, contrast enhanced, and the pixel gain (gamma) has been increased by a factor of 2 to better show the lower luminosity features of the leaders. The altitude scales in Figure 16 are referenced to the local coordinate system origin. The downward leader is imaged in frame 2, in addition to an upward connecting leader. The tips of both leaders and the top of the rocket tubes are annotated in Figure 16a with arrows. In Figure 16b, we have shown the subtraction of frame 1 from frame 2 with a compressed altitude scale to better depict the downward and upward leaders. The streamer zone of the downward leader was about 25 m in length and the upward connecting leader measured about 11.5 m in length. By increasing the pixel gain further, so as to see the details of the luminosity, we have determined that the faint luminosity between the bottom of the downward leader streamer zone and the upward leader tip is clearly the structure of rocket exhaust smoke illuminated by the converging leader channels, not the actual leader channel luminosity. At the end of the frame integration period, the bottom of the downward leader streamer zone and the upward leader tip were separated by about 28 m.

5. Discussion and Summary

[31] The "chaotic" dart leader process exhibits characteristics that differ from those of a typical dart leader or a typical dart-stepped leader. All four "chaotic" dart leaders recorded during summer of 2010 preceded return strokes with higher than average peak current, a finding in agreement with the results of *Bailey et al.* [1988] and *Rakov and Uman* [1990], in which return stroke peak electric field was used as a proxy for peak current. The features of the measured dE/dt waveforms of the order of tens of nanoseconds have not been previously documented. Furthermore, distinguishing "chaotic" dart leaders from other types of leaders, all four "chaotic" dart leaders followed periods of unusually long continuing current and unusually large charge transfer. The "chaotic" dart leader recorded during event UF 10–13 on 21 June 2010 followed the initial continuous current (ICC) resulting from the sustained upward positive leader that originated from the ascending triggering wire connecting to the cloud charge above. In this case, the ICC had duration of 680 ms and transferred about 68 C of negative charge to ground. The channel base current dropped to a level at or near zero for 100 ms between the end of the ICC and the first return stroke. The "chaotic" dart leaders recorded during the two triggered-lightning discharges on 15 July 2010 also immediately followed the ICC period after each respective wire launch. The ICC for event UF 10–20 had duration of 650 ms, transferring about 87 C of negative charge to ground. The channel base current dropped to a level at or near zero for 69 ms between the end of the ICC and the first return stroke. The ICC for event UF 10–21 had duration of 395 ms, transferring 42 C of negative charge to the ground. The channel base current dropped to a level at or near zero for 95 ms following the ICC. Both the duration of the ICC periods and charge transfers for these three events were larger than the means reported by *Wang et al.* [1999a] (GM) duration of 279 ms and GM charge transfer of 27 C) and by *Miki et al.* [2005] (GM duration of 305 ms and GM charge transfer of 30.4 C) for triggered-lightning discharges at the ICLRT. Interestingly, the channel base current dropped to a level at or near zero during the wire explosion (producing the so-called initial current variation) for all three of these events. This is not always the case [e.g.,

Olsen et al., 2006]. Finally, the "chaotic" dart leader recorded during event UF 10–24 on 13 August 2010 occurred after an interstroke continuing current of 135 ms duration following the second return stroke of the flash. This interstroke continuing current transferred about 15 C of negative charge to ground. The channel base current dropped to a level at or near zero for 45 ms at the end of the interstroke continuing current and before the initiation of the third return stroke.

[32] The dE/dt signatures of the four "chaotic" dart leaders recorded during summer 2010 shared some similar characteristics. The slower, but sub-microsecond, background field changes termed "bursts" in sections 4.1 and 4.2 were evident in all four "chaotic" dart leader dE/dt records. However, the relatively continuous trains of pulses superimposed on the bursts were only clearly evident and easily locatable via TOA techniques for events UF 10–13 and UF 10–24, which were also the two events preceding the stronger peak current return strokes (43.1 kA and 28.3 kA, respectively). The peaks of each burst and only a small number of pulses were locatable via TOA techniques for events UF 10–20 and UF 10–21, probably due to low system sensitivity, although the energetic radiation emission of both events was characteristic of a "chaotic" dart leader. The fact that the estimated source locations of the pulses tend to bounce up and down in altitude over a distance of often 5 to 30 m as the leader descends, coupled with the straight-line velocity between successive pulses often exceeding the speed of light, suggests that the leader is emitting pulses of high-frequency electric field radiation from multiple altitudes along the channel nearly simultaneously. This view is perhaps supported by the longer streamer zones (measured up to 25 m in length) of the "chaotic" dart leaders than those of typical dart leaders and dart-stepped leaders, the latter typically displaying a more fan-shaped characteristics and often including such luminous features as space stems/leaders [e.g., *Biagi et al.*, 2010].

[33] The trains of narrow dE/dt pulses recorded during the four "chaotic" dart leaders are generally dissimilar in both waveshape and interpulse interval from dart-stepped leader pulses. However, the energetic radiation (X-rays and gamma rays) recorded from all four "chaotic" dart leaders might be expected from a very rapid stepping process. For the nearly continuous emission of energetic radiation to be supported, the electric field intensity at or near the tip of the "chaotic" dart leader must remain nearly continuously at a level similar to that which occurs every microsecond or so in the bottom hundreds of meters of the propagation of a dart-stepped leader, where energetic radiation appears to be only emitted in close time correlation with the formation of a new leader step. If dE/dt sources are being emitted from multiple altitudes near the tip of the "chaotic" dart leader, it is reasonable that the source region for the energetic radiation detected in association with the descending leader is often some tens of meters in vertical extent at any instance in time, possibly resulting in the pronounced pileup of energetic photons within 5 μs of the subsequent return stroke that was observed for all four "chaotic" dart leader events.

[34] For both events UF 10–13 and UF 10–24, there appear to have been upward positive leaders initiated about 5 μs prior to the return stroke. From correlated channel base current records and TOA locations of the fast-transition pulses, which are assumed to correspond to the connection (s) of the upward and downward leaders, the upward leaders traversed distances of about 20 m at an average velocity of 3.7×10^6 m/s and about 30 m at an average velocity of 5.8×10^6 m/s for events UF 10–13 and UF 10–24, respectively.

[35] The findings of *Weidman* [1982], *Willett et al.* [1990], *Davis* [1999], *Gomes et al.* [2004], *Mäkelä et al.* [2007], and *Lan et al.* [2011] suggest that the "chaotic" component of descending leaders preceding subsequent return strokes may have duration from several tens of microseconds up to a half of a millisecond. For the four events discussed in this article, the "chaotic" component of the leader phase was only detected during the final 10 to 12 μs prior to the return stroke fast-transition pulses and was only sufficiently above the system noise level for suitable analysis for the final 6 μs prior to the return stroke. The short duration of the observed "chaotic" component compared to prior studies is likely a result of our relatively low system sensitivity. The dE/dt measurement sensitivities are configured to resolve both leader-step and return-stroke field changes from close distance (within 500 m) and low altitude. The fact that significant pulses of energetic radiation were detected up to about 13 μs prior to the return stroke suggests that the leaders likely had "chaotic" components from higher altitude. Energetic radiation measurements from higher altitude sources are restricted by a combination of atmospheric attenuation and system sensitivity.

[36] **Acknowledgments.** This research was partially supported by DARPA grants HR0011-08-1-0088 and HR0011-1-10-582 1–0061 and NASA grant NNK10MB02P.

References

Bailey, J., and J. C. Willett (1989), Catalog of absolutely calibrated, range normalized, wideband, electric field waveforms from located lightning flashes in Florida: July 24 and August 14, 1985 data, *NRL Memo. Rep. 6497*, 17 pp., Naval Res. Lab., Washington, D. C., 1 August.

Bailey, J., J. C. Willett, E. P. Krider, and C. Leteinturier (1988), Submicrosecond structures of the radiation fields from multiple events in lightning flashes, paper presented at 8th International Conference on Atmospheric Electricity, Inst. of High Voltage Res., Uppsala, Sweden.

Biagi, C. J., M. A. Uman, J. D. Hill, D. M. Jordan, V. A. Rakov, and J. Dwyer (2010), Observations of stepping mechanisms in a rocket-and-wire triggered lightning flash, *J. Geophys. Res.*, *115*, D23215, doi:10.1029/2010JD014616.

Davis, S. M. (1999), Properties of lightning discharges from multiple-station wideband electric field measurements, PhD dissertation, Univ. of Fla., Gainesville.

Dwyer, J. R., et al. (2003), Energetic radiation produced during rocket triggered lightning, *Science*, *299*, 694–697, doi:10.1126/science.1078940.

Dwyer, J. R., et al. (2004), Measurements of X-ray emission from rocket triggered lightning, *Geophys. Res. Lett.*, *31*, L05118, doi:10.1029/2003GL018770.

Dwyer, J. R., M. Schaal, H. K. Rassoul, M. A. Uman, D. M. Jordan, and D. Hill (2011), High-speed X-ray images of triggered lightning dart leaders, *J. Geophys. Res.*, *116*, D20208, doi:10.1029/2011JD015973.

Gomes, C., V. Cooray, M. Fernando, R. Montano, and U. Sonndara (2004), Characteristics of chaotic pulse trains generated by lightning flashes, *J. Atmos. Sol. Terr. Phys.*, *66*, 1733–1743, doi:10.1016/j.jastp.2004.07.036.

Guo, C., and E. Krider (1985), Anomalous light output from lightning dart leaders, *J. Geophys. Res.*, *90*, 13,073–13,075, doi:10.1029/JD090iD07p13073.

Howard, J., M. A. Uman, J. R. Dwyer, D. Hill, C. Biagi, Z. Saleh, J. Jerauld, and H. K. Rassoul (2008), Co-location of lightning leader X-ray and electric field change sources, *Geophys. Res. Lett.*, *35*, L13817, doi:10.1029/2008GL034134.

Howard, J., M. A. Uman, C. Biagi, D. Hill, J. Jerauld, V. A. Rakov, J. Dwyer, Z. Saleh, and H. Rassoul (2010), RF and X-ray source locations during the lightning attachment process, *J. Geophys. Res.*, *115*, D06204, doi:10.1029/2009JD012055.

Izumi, Y., and J. C. Willett (1993), Catalog of absolutely calibrated, range normalized, wideband, electric field waveforms from triggered lightning flashes in Florida, *Rep. P-TR-93-2151*, Phillips Lab., Dir. of Geophys., Hanscom AFB, Mass., 22 June.

Jerauld, J. E. (2007), Properties of natural cloud-to-ground lightning inferred from multiple-station measurements of close electric and magnetic fields and field derivatives, PhD dissertation, Univ. of Fla., Gainesville. [Available at http://purl.fcla.edu/fcla/etd/UFE0021279.]

Jerauld, J., M. A. Uman, V. A. Rakov, K. J. Rambo, and G. H. Schnetzer (2007), Insights into the ground attachment process of natural lightning gained from an unusual triggered-lightning stroke, *J. Geophys. Res.*, *112*, D13113, doi:10.1029/2006JD007682.

Jordan, D. M., V. P. Idone, V. A. Rakov, M. A. Uman, W. H. Beasley, and H. Jurenka (1992), Observed dart leader speed in natural and triggered lightning, *J. Geophys. Res.*, *97*, 9951–9957, doi:10.1029/92JD00566.

Koshak, W. J., et al. (2004), North Alabama lightning mapping array (LMA): VHF source retrieval algorithm and error analyses, *J. Atmos. Oceanic Technol.*, *21*, 543–558, doi:10.1175/1520-0426(2004)021<0543:NALMAL>2.0.CO;2.

Krider, E. P., C. D. Weidman, and R. C. Noggle (1977), The electric field produced by lightning stepped leaders, *J. Geophys. Res.*, *82*, 951–960, doi:10.1029/JC082i006p00951.

Lalande, P., A. Bondiou-Clergerie, P. Laroche, A. Eybert-Berard, J.-P. Berlandis, B. Bador, A. Bonamy, M. Uman, and V. Rakov (1998), Leader properties determined with triggered lightning techniques, *J. Geophys. Res.*, *103*, 14,109–14,115, doi:10.1029/97JD02492.

Lan, Y., Y. Zhang, W. Dong, W. Lu, H. Liu, and D. Zheng (2011), Broadband analysis of chaotic pulse trains generated by negative cloud-to-ground lightning discharge, *J. Geophys. Res.*, *116*, D17109, doi:10.1029/2010JD015159.

Mäkelä, J. S., M. Edirisinghe, M. Fernando, R. Montaño, and V. Cooray (2007), HF radiation emitted by chaotic leader processes, *J. Atmos. Sol. Terr. Phys.*, *69*, 707–720, doi:10.1016/j.jastp.2007.01.003.

Miki, M., V. A. Rakov, T. Shindo, G. Diendorfer, M. Mair, F. Heidler, W. Zischank, M. A. Uman, R. Thottappillil, and D. Wang (2005), Initial stage in lightning initiated from tall objects and in rocket-triggered lightning, *J. Geophys. Res.*, *110*, D02109, doi:10.1029/2003JD004474.

Olsen, R. C., V. A. Rakov, D. M. Jordan, J. Jerauld, M. A. Uman, and K. J. Rambo (2006), Leader/return-stroke-like processes in the initial stage of rocket-triggered lightning, *J. Geophys. Res.*, *111*, D13202, doi:10.1029/2005JD006790.

Orville, R. E., and V. P. Idone (1982), Lightning leader characteristics in the Thunderstorm Research International Program (TRIP), *J. Geophys. Res.*, *87*, 11,177–11,192.

Rakov, V. A., and M. A. Uman (1990), Some properties of negative cloud-to-ground lightning flashes versus stroke order, *J. Geophys. Res.*, *95*, 5447–5453, doi:10.1029/JD095iD05p05447.

Rakov, V. A., and M. A. Uman (2003), *Lightning: Physics and Effects*, Cambridge Univ. Press, New York.

Saleh, Z., et al. (2009), Properties of the X-ray emission from rocket-triggered lightning as measured by the Thunderstorm Energetic Radiation Array (TERA), *J. Geophys. Res.*, *114*, D17210, doi:10.1029/2008JD011618.

Schonland, B. F. J., D. J. Malan, and H. Collens (1935), Progressive lightning II, *Proc. R. Soc. A*, *152*, 595–625, doi:10.1098/rspa.1935.0210.

Thomas, R. J., P. R. Krehbiel, W. Rison, S. J. Hunyady, W. P. Winn, T. Hamlin, and J. Harlin (2004), Accuracy of the lightning mapping array, *J. Geophys. Res.*, *109*, D14207, doi:10.1029/2004JD004549.

Wang, D., V. Rakov, M. Uman, M. Fernandez, K. Rambo, G. Schnetzer, and R. Fisher (1999a), Characterization of the initial stage of negative rocket-triggered lightning, *J. Geophys. Res.*, *104*, 4213–4222, doi:10.1029/1998JD200087.

Wang, D., N. Takagi, T. Watanabe, V. A. Rakov, and M. A. Uman (1999b), Observed leader and return-stroke propagation characteristics in the bottom 400 m of the rocket triggered lightning channel, *J. Geophys. Res.*, *104*, 14,369–14,376, doi:10.1029/1999JD900201.

Weidman, C. D. (1982), The submicrosecond structure of lightning radiation fields, PhD dissertation, Univ. of Ariz., Tucson.

Willett, J., J. Bailey, C. Leteinturier, and E. Krider (1990), Lightning electromagnetic radiation field spectra in the interval from 0.2 to 20 MHz, *J. Geophys. Res.*, *95*, 20,367–20,387, doi:10.1029/JD095iD12p20367.

J. R. Dwyer and H. Rassoul, Department of Physics and Space Sciences, Florida Institute of Technology, 150 W. University Blvd., Melbourne, FL 32901, USA.

J. D. Hill, D. M. Jordan, and M. A. Uman, Department of Electrical and Computer Engineering, University of Florida, PO Box 116200, Gainesville, FL 32611, USA. (gators15@ufl.edu)